Extraordinary climates of Earth-like planets: three-dimensional climate simulations at extreme obliquity

Darren M. Williams[1] and David Pollard[2]

[1]*School of Science, Penn State Erie, The Behrend College, Station Road, Erie PA 16563-0203, USA*
e-mail: *dmw145@psu.edu*
[2]*EMS Environment Institute, The Pennsylvania State University, University Park PA 16802, USA*
e-mail: *pollard@essc.psu.edu*

Abstract: A three-dimensional general-circulation climate model is used to simulate climates of Earth-like planets with extreme axial tilts (i.e. 'obliquities'). While no terrestrial-planet analogue exists in the solar system, planets with steeply inclined spin axes may be common around nearby stars. Here we report the results of 12 numerical experiments with Earth-like planets having different obliquities (from $0°$ to $85°$), continental geographies, and levels of the important greenhouse gas, CO_2. Our simulations show intense seasonality in surface temperatures for obliquities $\geqslant 54°$, with temperatures reaching $80–100\ °C$ over the largest middle- and high-latitude continents around the summer solstice. Net annual warming at high latitudes is countered by reduced insolation and colder temperatures in the tropics, which maintains the global annual mean temperature of our planets to within a few degrees of $14\ °C$. Under reduced insolation, seasonal snow covers some land areas near the equator; however no significant net annual accumulation of snow or ice occurs in any of our runs with obliquity exceeding the present value, in contrast to some previous studies. None of our simulated planets were warm enough to develop a runaway greenhouse or cold enough to freeze over completely; therefore, most real Earth-like planets should be hospitable to life at high obliquity.

Introduction

What would Earth's climate be like if its spin axis were inclined by much more than $23.5°$, as it is today? Simulating Earth's climate at high obliquity is interesting from a purely academic point of view, but it also helps us to understand the role obliquity and climate have played in the development of life here on Earth and on potentially habitable planets around nearby stars. The stochastic nature of terrestrial-planet accretion is likely to leave many Earth-like planets with spin axes inclined toward their orbital planes by more than $30°$ (Agnor *et al.* 1999). All of the terrestrial planets in our solar system have spin axes that are approximately parallel to their orbit normals (with obliquities $<30°$), but this may be attributed to either the tidal influence of the Sun, as in the case of Mercury and Venus (Alexandre & Laskar 2001), or chance. Earth's own obliquity could have originally been anywhere in the range $0°–180°$ as a consequence of the giant collisions occurring near the end of its accretion, one of which is thought to have formed the Moon (Canup & Agnor 2000).

An obliquity higher than $54°$ might explain the paradoxical evidence for ice-covered land areas within $\sim 20°$ of Earth's equator during the Late Precambrian (Evans *et al.* 1997; Williams & Schmidt 1998; Oglesby & Ogg 1998; Chandler & Sohl 2000; Jenkins 2000), but strong low-obliquity explanations for the tropical glaciations have also been offered, such as the 'snowball-Earth' hypothesis (Hoffman *et al.* 1998), with varying degrees of modelling support (Chandler & Sohl 2000; Hyde *et al.* 2000; Jenkins 2000, 2002). If Earth's spin axis were inclined by more than $54°$ in the Late Precambrian, then a mechanism would have been required to reduce Earth's obliquity from a hypothetically large primordial value to $23.5°$ over short geological timescales, but finding such a mechanism has proven difficult (cf. Williams 1993; N'eron de Surgy & Laskar 1997; Williams *et al.* 1998). Earth is effectively held upright at low obliquity by the strong gravitational influence of the Moon. A decade ago, Jacques Laskar and colleagues (Laskar & Robutel 1993; Laskar *et al.* 1993) demonstrated that Earth's axial tilt is stable with the Moon present for obliquities of less than $60°$. Without the Moon, Earth's obliquity would vary chaotically as a consequence of solar tides between $0°$ and $90°$ on timescales of less than 10 Myr. This result lead Laskar and colleagues to suggest that the Moon is in some sense *necessary* for the existence of life on

Earth because it stabilizes the spin axis at low obliquity and maintains climatic clemency over most of the planet. If true, the number of habitable planets in the Galaxy is, then, a fraction of the number of terrestrial planets with sizeable moons, which should be small if they form by accident as our Moon did.

It is now known that the obliquity variations found by Laskar for a moonless Earth will not plague every moonless terrestrial planet. The reason is twofold. First, in addition to the gravitational influence of the Sun and the Moon, obliquity is also affected by the precessional motion of a planet's orbital plane, which depends on the size and proximity of neighbouring planets (Williams 1998a; Ward *et al.* 2002). In the present solar system, Earth is more stable *with* the Moon because its spin axis precesses much faster than the orbit does in response to the distant planets. As a result, obliquity is held fixed to within a few degrees of 23.5°. However, if Jupiter were moved inward from 5.2 to 3.0 AU around the Sun, Earth's spin axis would be more stable *without* the Moon than with the Moon with all other parameters being equal. The stronger gravitational perturbations of Jupiter would cause Earth's orbit to precess more than twice as fast as it does today, which would bring the rates of orbital precession and precession of the spin axis for the moonless Earth into a close resonance. This would in turn increase the amplitude of the obliquity cycle and the chaotic behavior of the spin axis.

Moonless planets at high obliquity might still be habitable for another reason. The exact climatic response of a planet to high obliquity depends on many atmospheric and topographic parameters, such as the size and positions of continents and the concentrations of greenhouse gases. Williams & Kasting (1997) used an energy-balance model (EBM) to investigate the response of Earth's climate to high obliquity at different distances away from the Sun. For that study, it was found that summer-time temperatures over middle and high latitudes were in the 50–80 °C range with Earth at 1.0 AU and with obliquity set close to 90°. These temperatures are conservative values because they were obtained by averaging the temperatures over latitudinal bands including large amounts of ocean. Seasonal cycle amplitudes would have been considerably more amplified in the model had the continents been larger because continental interior temperatures respond much more rapidly to changes in seasonal insolation than ocean surface temperatures. Conversely, seasonal cycle amplitudes would be *smaller* on planets with less land or with continents confined to the tropics where insolation changes little over a seasonal cycle compared with at high latitude (see Fig. 1).

Williams & Kasting (1997) also found that some planets could have their seasonal cycles significantly reduced at high obliquity if they accumulate large amounts of CO_2 in their atmospheres (with $pCO_2 > 1$ bar) as a consequence of the carbonate–silicate weathering cycle. Such planets are expected to occupy the outer regions of their habitable zones where stellar flux and effective temperatures are lower. Dense CO_2 atmospheres transport heat efficiently away from warm areas while reducing rates of cooling for less insolated areas
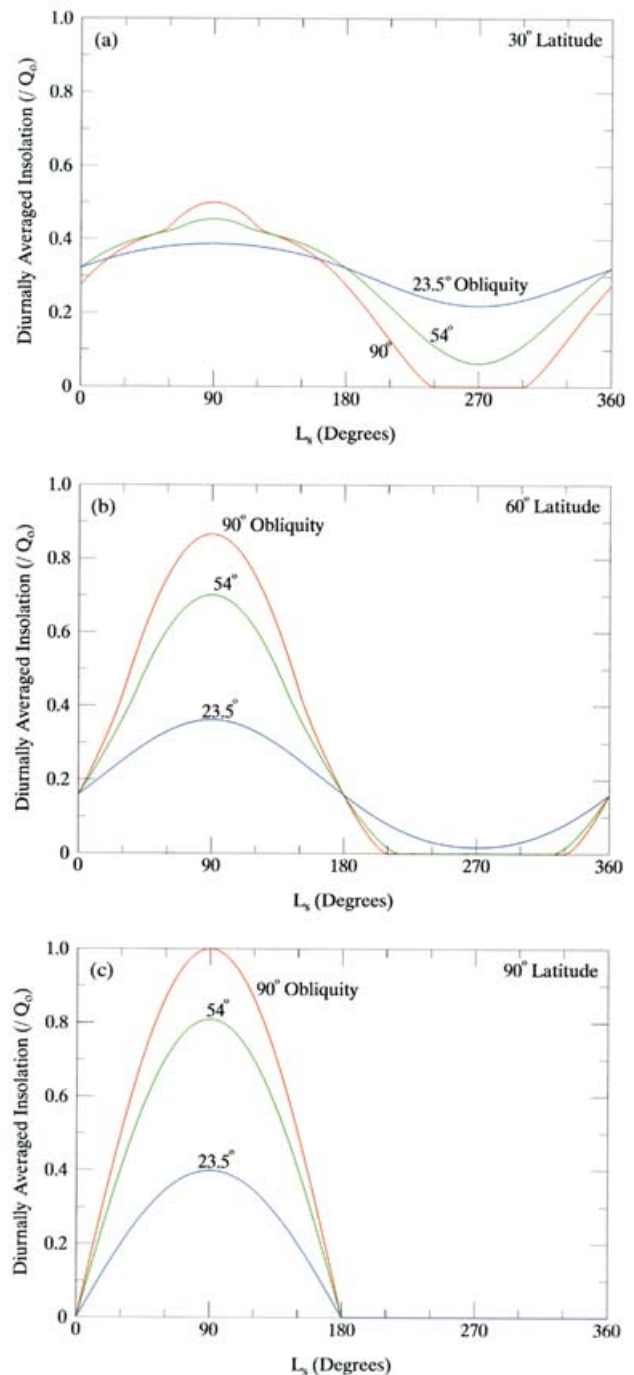

Fig. 1. Diurnally averaged insolation relative to the solar constant received by our planets at obliquities of 23.5° (blue), 54° (green) and 90° (red) for three different latitudes: (a) 30°, (b) 60° and (c) 90°. Insolation is plotted as a function of orbital longitude L_s, which is 0° and 180° at the vernal and autumnal equinoxes, respectively, and 90° and 270° at the summer and winter solstices. The solar constant $Q_0 = 1370$ W m^{-2} and the global-mean insolation is $Q_0/4$.

through the greenhouse effect. Unfortunately, the dense atmospheres studied previously with the EBM cannot yet be simulated in three dimensions because the infrared radiation code in the climate model employed for this study becomes
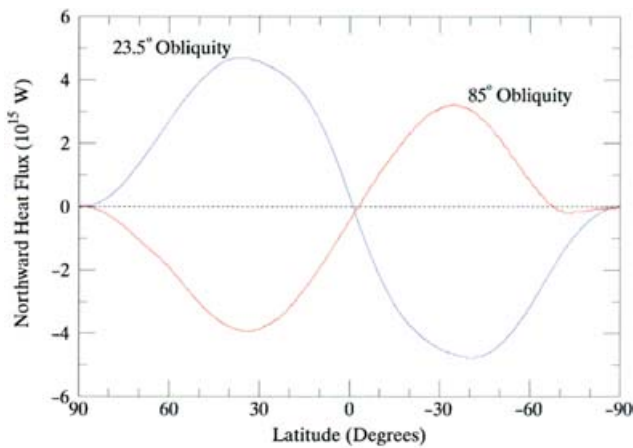
Fig. 2. Total annual northward atmospheric and oceanic heat flux in watts for runs PRES23, with 23.5° obliquity, and PRES85, with 85° obliquity. In our model, energy is transported across zonal boundaries by winds and by diffusive heat flow in the 50 m deep wind-mixed ocean layer.

increasingly inaccurate for CO_2 concentrations above $\sim 10 \times$ PAL (present atmospheric level; 1 PAL = 350 ppm).

So we will focus our attention here on planets with thin atmospheres and Earth-like surfaces with similar land–sea ratios, some with familiar continents and others with alien landscapes. The primary purpose of this work is to extend the earlier work of Williams and Kasting using a model of greater sophistication and predictive power to learn how planetary climate responds to parameters such as continental topography and obliquity. The results of our simulations might then be used to make informed statements regarding the existence of life on planets that are either similar to, or vastly different, from Earth.

Previous GCM runs at high obliquity

Earth general-circulation modelling (GCM) experiments with high obliquities have been performed by Hunt (1982), Williams (1988b, c), Oglesby & Ogg (1998), Chandler & Sohl (2000) and Jenkins (2000, 2001, 2003) using a wide range of paleocontinental distributions, solar constant reductions and atmospheric CO_2 levels. All of these studies found that low latitudes cool with large obliquities, and some cases achieve a 100% snowball earth. Oglesby & Ogg (1998) and Jenkins (2000) found other cases with permanent snow and ice in low latitudes ($\sim 30°$ S to 30° N) and not at higher latitudes. A common feature in high-obliquity simulations is the reversal in meridional (north–south) heat flow *toward* the equator, rather than *away* from it as on the present Earth. This reversal stems from the poles receiving more insolation on average than the tropics at an obliquity above 54°. In our model, heat transport is accomplished both by advection within the atmosphere and diffusion in the 50 m slab ocean and is shown to be away from the poles at high obliquity in Fig. 2. According to Fig. 2, approximately 5×10^{15} W of energy is transported away from Earth's tropics by winds and ocean

Table 1. *Planetary parameters used in the GCM runs (columns 1–5), along with global annual-mean temperatures (column 7) obtained from the model results. Geographies for 750 Ma (Sturtian) and 540 Ma (close to Varanger) were derived from paleogeographic reconstructions by Lawver et al. (1999) for the Late Proterozoic era of Earth's history. Carbon dioxide partial pressures are given in ppmv (parts per million by volume). All runs were performed with Earth at 1.0 AU around the Sun and in its present orbit with eccentricity = 0.0167. Solar luminosity is given in column 4 relative to the present output. Column 6 lists the figures with global maps of each run*

Run	Geography	Obliquity (deg)	Luminosity ($L_\odot$)	pCO_2 (ppmv)	Figures	T_{ave} (°C)
PRES23	Present	23.5	1.0	345	3–7	14.0
PRES54	Present	54	1.0	345	–	17.6
PRES70	Present	70	1.0	345	–	16.4
PRES85	Present	85	1.0	345	9–12	15.5
HICO2:23	Present	23.5	1.0	3450	–	23.6
HICO2:54	Present	54	1.0	3450	–	23.2
HICO2:70	Present	70	1.0	3450	–	21.9
HICO2:85	Present	85	1.0	3450	14	20.6
PRES0	Present	0	1.0	345	15	11.2
STUR0	Sturtian	0	1.0	345	15	7.2
STUR85	Sturtian	85	0.94	420	17–19	16.0
VARA85	Varanger	85	0.94	420	20–22	13.3

currents and is deposited northward of 30° latitude each year. Meridional heat transport, then, accounts for $\sim 1/8$ of the net annual energy budget (relative to solar insolation) for this region of the planet, which illustrates how important a robust treatment of heat transport is to accurately model climates in three dimensions and at high obliquity.

Model description

The three-dimensional climate model used for this study is GENESIS 2 (Thompson & Pollard 1997; Pollard & Thompson 1995), which is the same model used previously to simulate the climates of Earth-like planets on orbits of extreme eccentricity (Williams & Pollard 2002). GENESIS 2 is a general circulation model coupled to multi-layer surface models of vegetation, soil, land ice, snow and a 50 m slab ocean layer with dynamic sea ice. The atmospheric model uses spectral transform dynamics for mass, heat and momentum, and semi-Lagrangian transport in grid space for water vapour and other tracers including isotopes. Other significant features include a diurnal cycle, an explicit sub-grid buoyant plume model of convection and prognostic cloud water amounts. The land-surface model includes two vegetation layers (trees and grass) through which radiative and turbulent fluxes are calculated. Rain or snow can be intercepted by the vegetation and re-evaporated. A six-layer soil model extends from the surface to 4 m depth, and includes vertical heat diffusion, liquid water transport, surface runoff, bottom drainage, uptake of liquid water by plant roots for transpiration, and the freezing and thawing of soil ice. The atmospheric grid
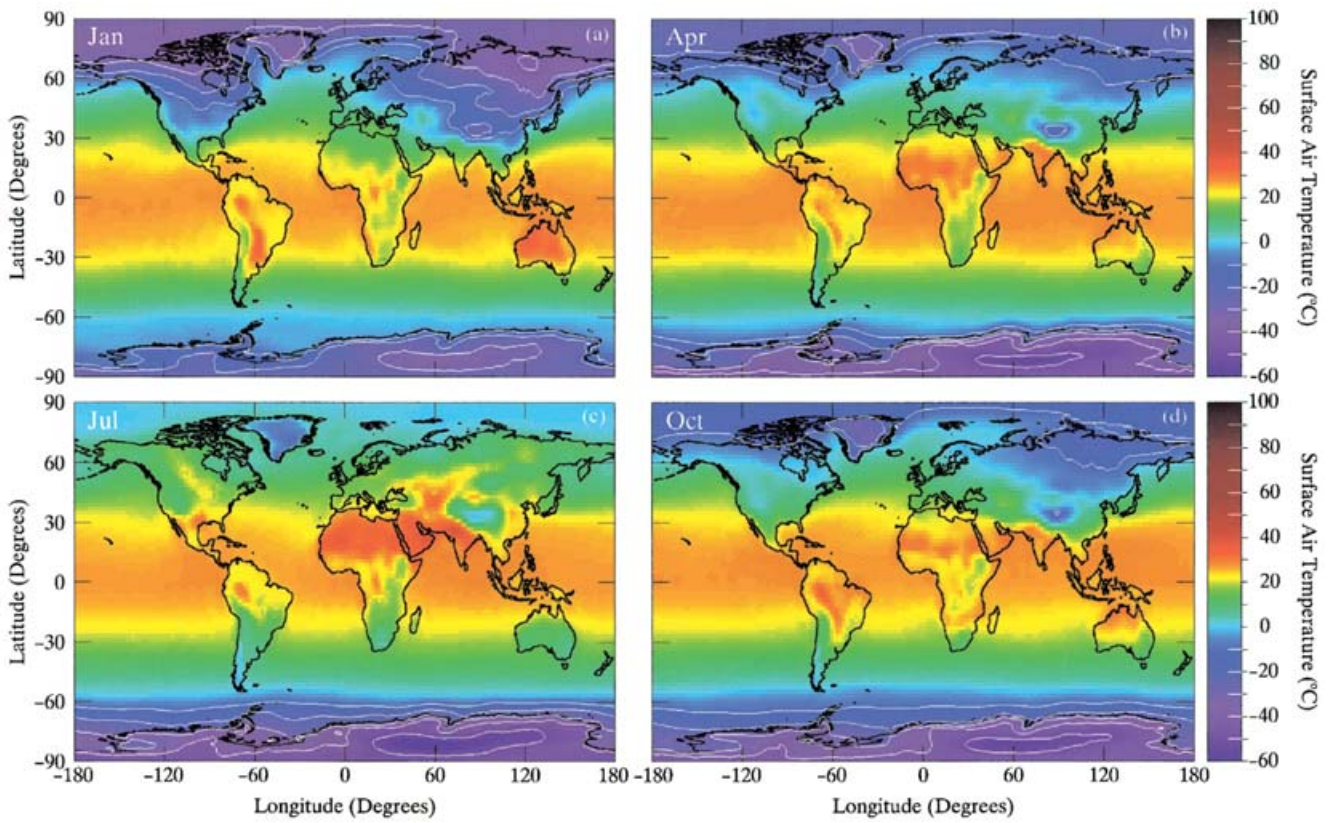
Fig. 3. Monthly mean 2 m surface air temperatures (°C) for run PRES23. White contours on the colour bars and on the maps mark temperatures $\leqslant -10\,°C$ and $\geqslant 50\,°C$ in 10° intervals. Maps are shown for the months of January, April, July and October.
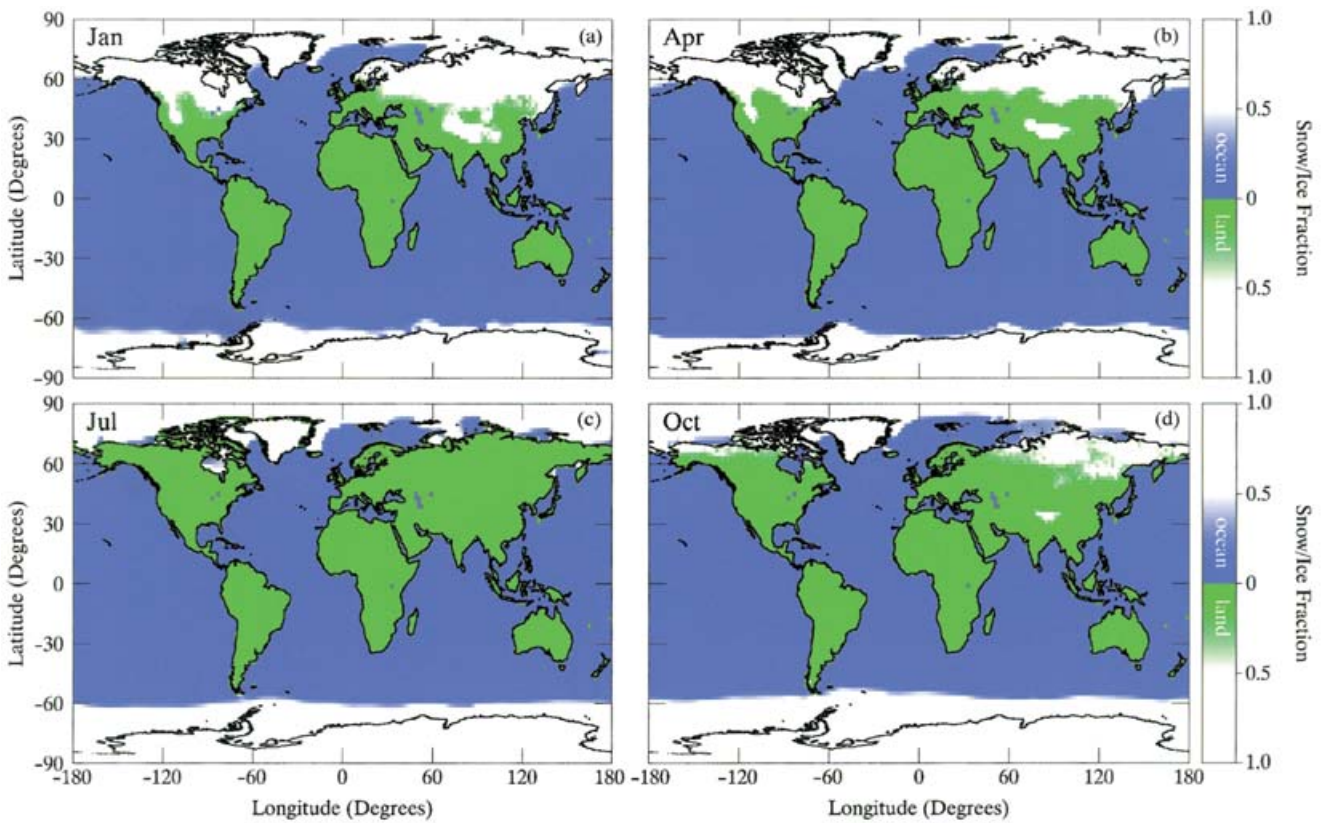

Fig. 4. Distribution of ice and snow for the months of January, April, July and October for run PRES23. Land surfaces having a snow/ice fraction $<50\%$ are shaded green and ocean surfaces having a snow/ice fraction $<50\%$ are shaded blue.
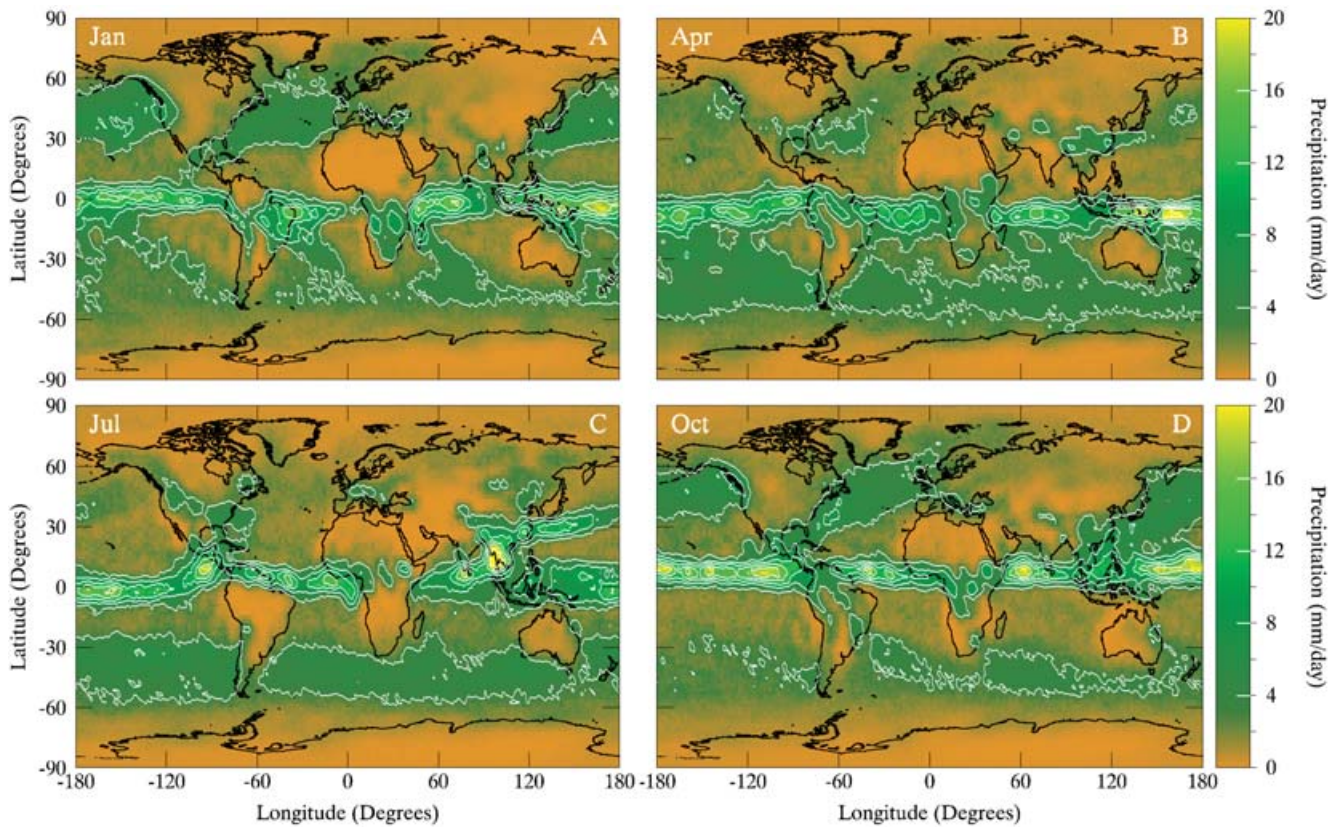
Fig. 5. Monthly mean precipitation in mm d^{-1} for the months of January, April, July and October for run PRES23. White contours on the colour bars and on the maps mark precipitation levels in steps of 4 mm d^{-1}.
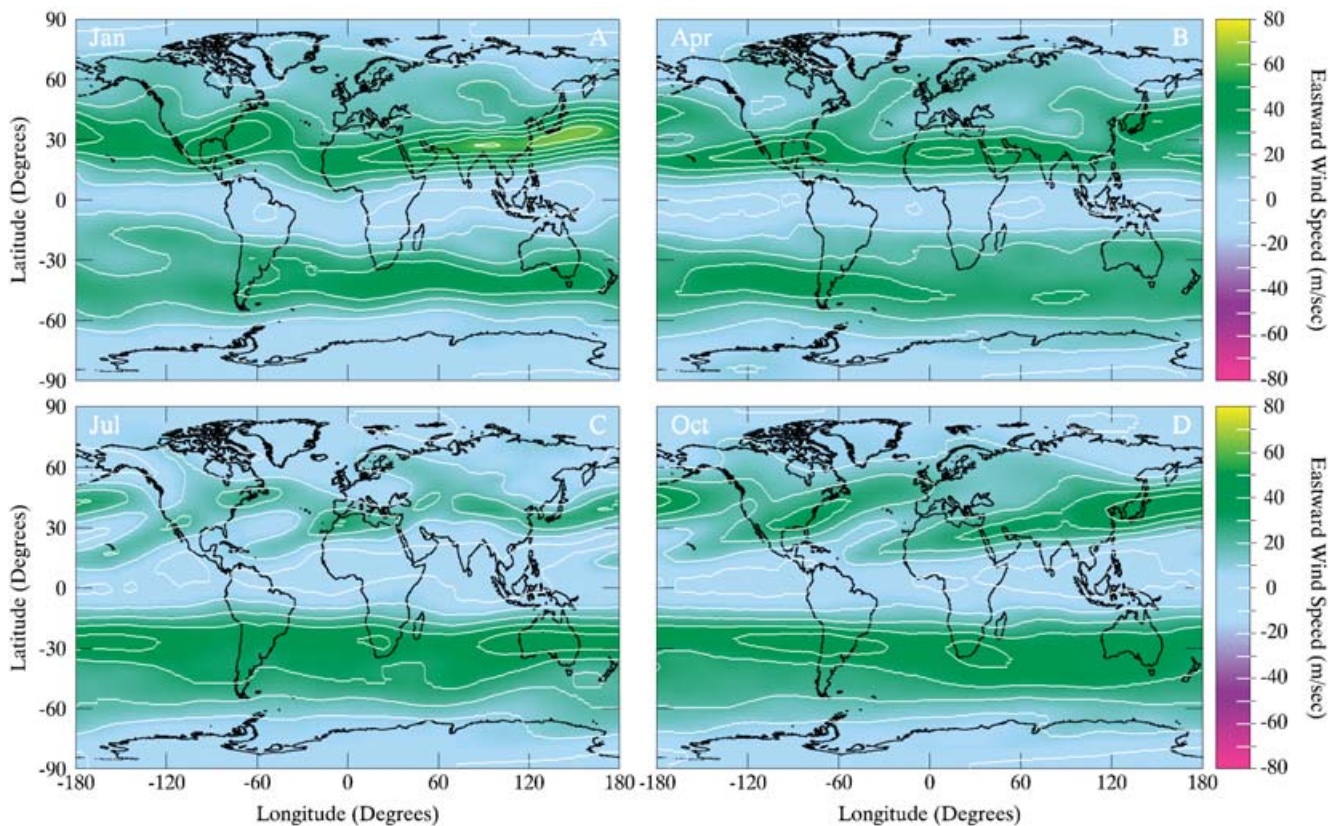

Fig. 6. Monthly mean eastward wind speed in m s^{-1} at a sigma level (P/P_0) of 0.251, or a height of $\sim$10 km above the surface. Shown are maps for the months of January, April, July and October for run PRES23. White contours on the colour bars and on the maps mark velocity levels in steps of 20 m s^{-1}.
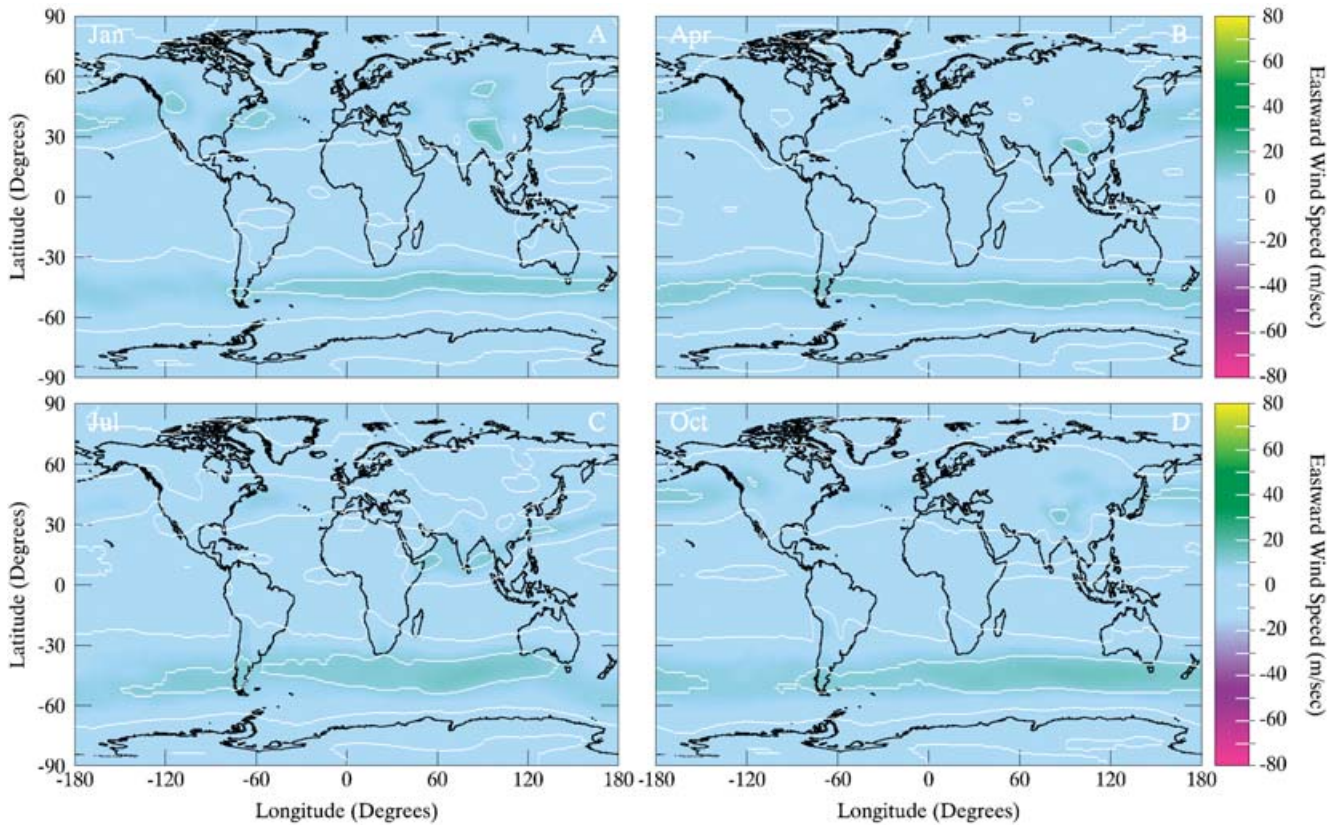
Fig. 7. Monthly mean eastward wind speed in m s^{-1} at a sigma level (P/P_0) of 0.866, or a height of ~ 1 km above the surface, for run PRES23.

is spectral T31 (3.75×3.75 deg^2) with 18 vertical levels and the grid for all surface models is 2×2 deg^2. All GCM experiments were performed on CRAY supercomputers and convergence was reached after ~ 30 model years, lasting ~ 1000 CPU hours.

Results

Climate at high obliquity

The first thing we did with the GENESIS 2 GCM was raise the obliquity of Earth to 54°, 70° and then 85° while holding all other run parameters equal to their normal values for the present Earth. These three runs are labeled PRES54, PRES70 and PRES85 in Table 1. To enable an easy comparison between our new results and those for present Earth we also include here the results of a control run, PRES23 (Thompson & Pollard 1997). For each simulation, monthly means of many variables were saved, including: 2 m air surface temperature, precipitation and evaporation rates, snow fraction over land and ice, sea-ice fraction over oceans, and eastward and northward wind speeds at three atmospheric sigma levels (P/P_0, where P is the pressure and P_0 is the surface pressure): 0.251, 0.501 and 0.866, which correspond to approximate heights of 1, 5 and 10 km above the surface respectively. For run PRES23, we show global maps (Figs 3–7) of temperature, snow/ice coverage, precipitation and eastward wind velocities (1 and 10 km only) for the months immediately following
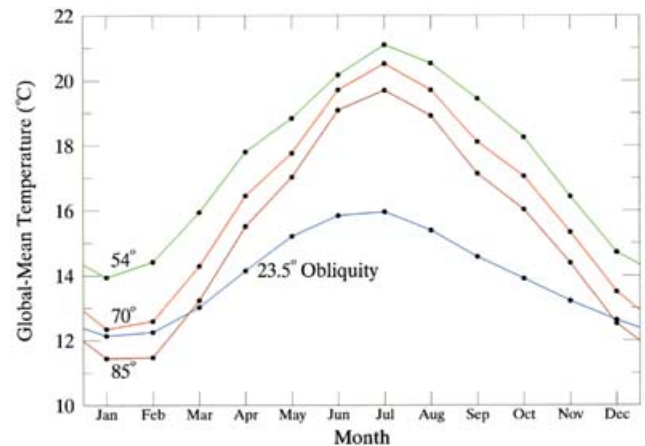

Fig. 8. Seasonal variation of global-mean temperature (in °C) for the present Earth with several different obliquities. Runs graphed here include PRES23 (23.5° obliquity), PRES54 (54°), PRES70 (70°) and PRES85 (85°) using blue, green, orange and red colours, respectively.

the solstices and equinoxes on Earth (January, April, July, October). Maps of meridional (north–south) wind speed are not shown because the speeds were found not to vary much above 10 m s^{-1} (~ 22 mph), even under the most extreme circumstances. Table 1 lists the global annual-mean temperature and Fig. 8 shows the seasonal cycle for the global monthly mean temperature.
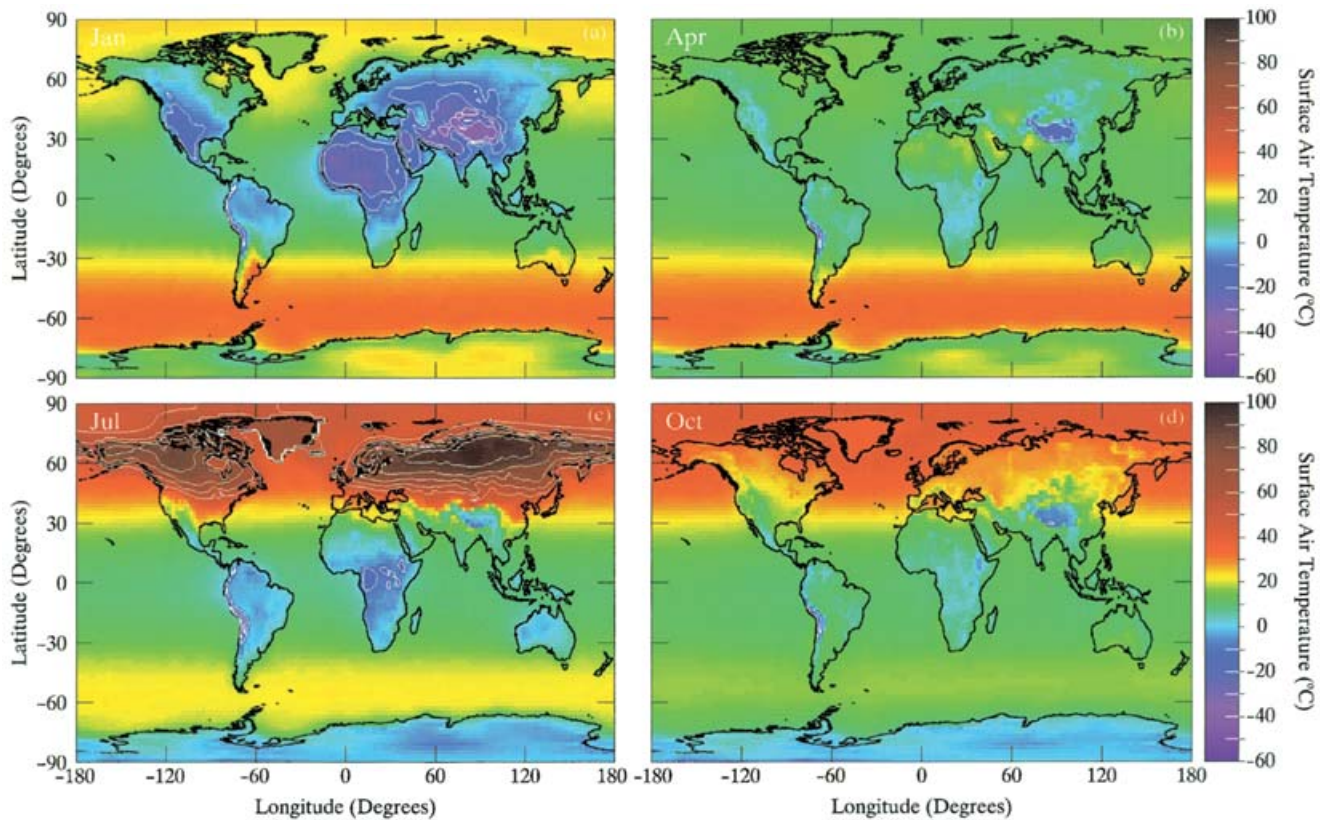
Fig. 9. Monthly mean 2 m surface air temperatures (°C) for run PRES85. Compare with Fig. 3.

For the present-day control run, PRES23, the model captures most of the important features of Earth's present climate reasonably well, including snow and ice coverage and regional precipitation patterns such as the Saharan drought and the seasonal monsoons over southeast Asia (Fig. 5), as well as the strong mid-latitude eastward jets at ~10 km altitude. As observed, winds closer to the ground are much weaker than those aloft. Consequently, we limit the wind results shown below to the 10 km level, which shows the greatest differences for planets at high obliquity.

Fig. 8 compares global temperature cycles for a wide range of obliquities. From this figure and Table 1, it is apparent that obliquities greater than the present (PRES54, PRES70 and PRES85) produce global annual-mean temperatures higher than Earth's present mean temperature of 14.0 °C. Above 54° obliquity with present geography, the trend is for the global annual-mean temperature to decrease as obliquity increases: from 17.6 °C at 54° obliquity, to 16.4 °C at 70° obliquity, and lastly to 15.5 °C at 85° obliquity.

Before explaining this trend, it is important to remember that global annual-mean temperature would be independent of obliquity if a planet were topographically uniform. In cases where there is a mix of land and ocean, the exact climatic response to different obliquities will depend on the sizes and locations of continents because the planetary albedo is strongly influenced by the distribution of ice and snow and by the height of the Sun over water-covered surfaces.

The slight decline in temperature as obliquity increases results from a disproportionate amount of land above 30° N latitude on the present Earth. Here, elevated annual insolation warms the surface enough (Figs 9 and 10) to prevent accumulation of snow and to melt present-day ice-sheets covering Greenland and Antarctica. (We did not remove these ice sheets in the GCM runs. For the PRES series of runs, the ice would have disappeared given the extreme summer temperatures over the poles, so we crudely corrected air temperatures over these areas in the displayed maps as follows: temperatures over Greenland were set equal to those near sea level in central-northern Canada, and model temperatures over the Antarctic ice sheet were reduced to sea level using topographic data and an atmospheric lapse rate of 6.5 °C km^{-1}.) The disappearance of snow and ice at high latitude is responsible for lowering the planetary albedo and raising the global annual-mean temperature 3.6 °C from run PRES23 to PRES54. The subsequent decline in global annual-mean temperature as obliquity is increased further is caused by the Sun spending less time overhead in the tropics, which reduces the incident insolation at low latitudes. Thus, the tropics are naturally colder at high obliquity, but low-latitude temperatures are reduced even further by the greater reflectivity of the oceans when the Sun is nearer the horizon. The amount of cooling, then, depends sensitively on the percentage of the surface covered by oceans, which is approximately 70 % for the region between 30° S and 30° N on the present Earth.
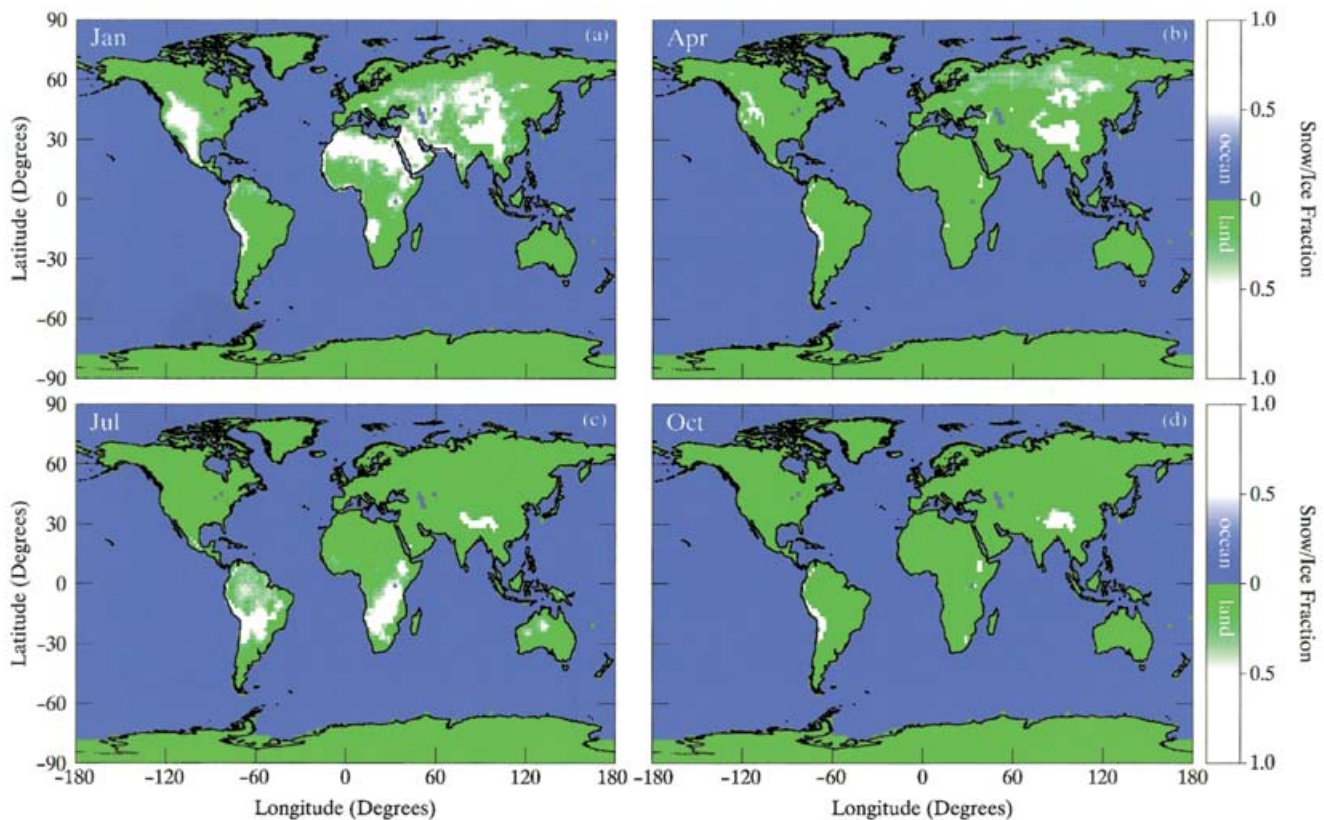
Fig. 10. Seasonal distribution of ice and snow for run PRES85. Compare with Fig. 4.

With half of the Earth's surface lying within 30° of the equator, the cooler tropics result in a lower global-mean temperature despite the elevated temperatures (reaching 80–100 °C in July over the northern continents) at high latitudes. Fig. 9 shows that temperatures over the equatorial oceans seasonally hover around 10 °C at 85° obliquity. Although no sea ice forms at low latitude for this set of runs, ice would likely cover the equatorial ocean as it does in the Arctic today under a reduced solar constant or smaller amounts of CO_2. Also, snowfall occurs at low latitudes and high elevations as expected (Fig. 10). Most interesting is the seasonal snow coverage stretching from northern Africa over the modern Sahara through the Middle East. The only locations that snow is able to persist year round are in the Andes Mountains of western South America and in the extreme highlands of eastern Africa. And although these are possible sites for the formation of glaciers, the areas covered by ice are detached and considerably smaller than the large ice sheets covering landmasses in the tropics in runs performed by Oglesby & Ogg (1998) and Jenkins (2000). This also supports the idea that ice sheets are difficult to form in the tropics at any obliquity with CO_2 as high as it is today.

The reason why snow falls in northern Africa (for example) at high obliquity is because the temperatures are colder, and because global precipitation patterns have changed (compare Figs 5 and 11). The most significant changes at high obliquity are the absence of the inter-tropical convergence zone (the band of high-intensity rainfall in Fig. 5) and the seasonal

delivery of moisture to normally drought-stricken areas such as the Sahara.

These dramatic changes in precipitation are enabled by a reorganization of the global circulation, which at high obliquity would blow to the west, opposite to the normal flow (compare Figs 6 and 12). The reversal in wind direction stems from the reversal in climatic zonation once obliquity exceeds 54°. In this case, heat is transported equatorward rather than poleward (see Fig. 2) so that the Hadley circulation is reversed; dense cold air moves *away from* the equator near the surface while warmer air from the poles moves *toward* the equator aloft. The high-altitude winds moving toward the equator are deflected to the left (west) by a Coriolis force, rather than to the right (east) as they move away from it. This sets up the strong westward wind current seen in Fig. 12.

The second important change that results from a reversed Hadley circulation on planets at high obliquity is the removal of the inter-tropical convergence zone, which on Earth results from cold surface air from both hemispheres meeting at the equator, being warmed and moistened, and ascending to create thunderstorms. On the high-obliquity Earth, air at the equator is descending rather than ascending, and precipitation is reduced (compare Figs 5 and 11).

Another major difference between the planet in run PRES85 and the present Earth is the extreme summertime drought affecting the entire planet surface poleward of 40° N (Fig. 11c). This drought is due to the extreme summertime heating of the lower atmosphere, with temperatures over
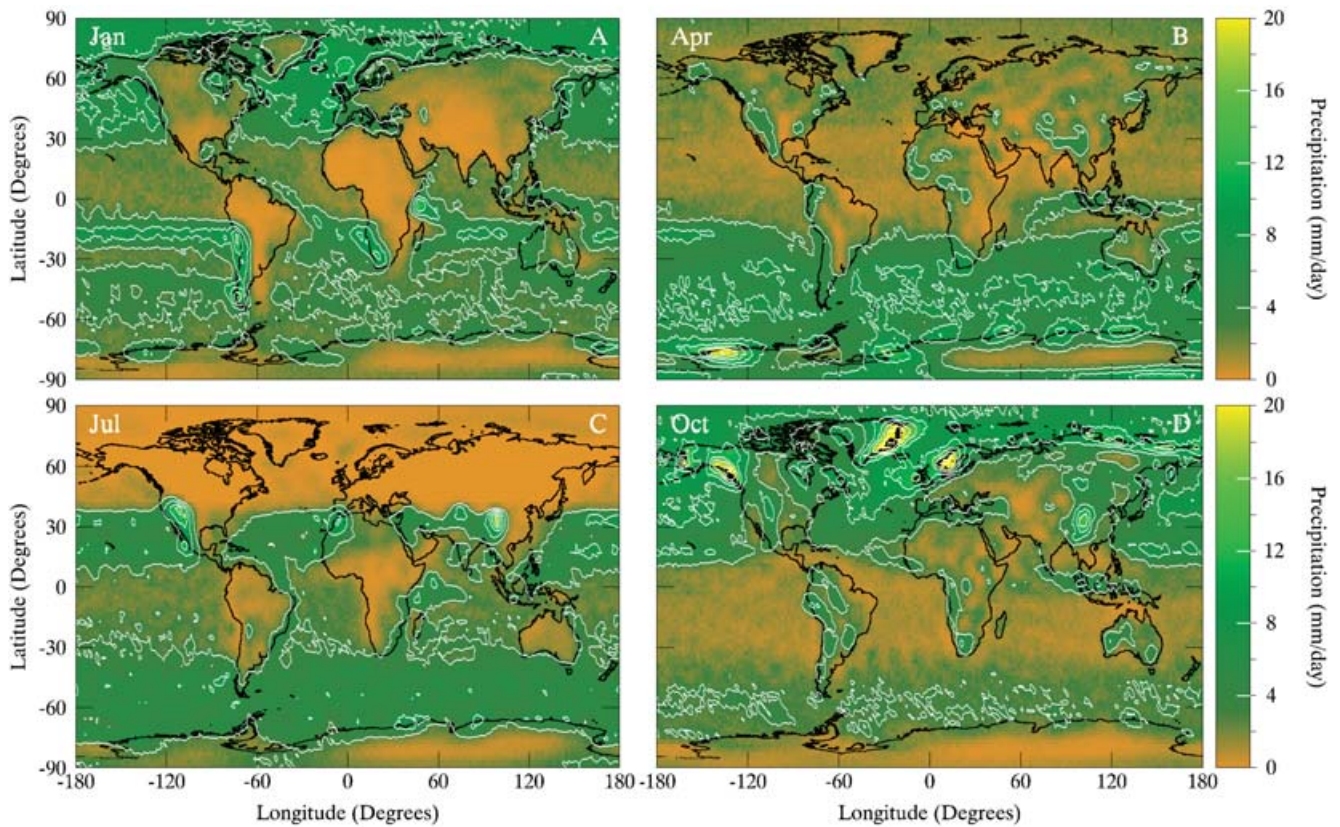
Fig. 11. Monthly mean precipitation in mm d^{-1} for run PRES85. Note the extreme July drought. Compare with Fig. 5.

Northern Canada and Russia (see Fig. 9) reaching 80–90 °C! Although this heating enhances surface evaporation rates, especially over the North Atlantic and Arctic oceans, precipitation is actually reduced in the warm troposphere because the saturation water-vapour pressure always exceeds the actual vapour pressure (i.e. the relative humidity remains low), which suppresses condensation. This summertime dry spell is seen in all of our runs where surface temperatures exceed 50 °C.

Raising pCO_2

The next thing we did with the GENESIS 2 GCM was to repeat the PRES series of runs, but with pCO_2 increased to 10 times the present level, or 3450 ppm. The level of carbon dioxide in the Earth's early atmosphere is not well constrained and may have been anywhere between 100 ppm and a few bars (Kasting 1992). Concentrations exceeding 0.1 bars may have been needed to keep the early Earth unfrozen under a less luminous Sun. Concentrations of similar greenhouse gases in the atmospheres of putative extrasolar terrestrial planets are even less constrained because they depend on many planetary and astronomical parameters affecting how planets acquire and hold on to volatiles. We would have liked to have modelled planets with CO_2 concentrations above 1 bar since the amplitudes of the seasonal temperature at high obliquity are expected to be smaller and, thus, less problematic for life (Williams & Kasting 1997). But 3450 ppm is the highest concentration that our model could

handle accurately, so we chose that value for runs HICO2:23–HICO2:85 (see Table 1).

As expected, temperatures for this set of runs are higher than for the earlier runs with present CO_2, with increases in global annual-mean temperatures of between 6 and 10 °C (Table 1). Above 54° obliquity, temperatures follow the same downward trend as before as obliquity is increased but with one important difference. A comparison of Figs 8 and 13 reveals that Earth is coldest at 23.5° obliquity with pCO_2 at the present level. However, raising pCO_2 to 3540 ppm results in Earth being warmer at 23.5° obliquity than at higher obliquity. The reason is that Earth's surface is presently cold enough to sustain ice and snow at the poles year round, which raises the planetary albedo and cools the surface even further. A sharp temperature transition occurs between run PRES23 and PRES54 because the permanent and semi-permanent snow–ice cover is significantly reduced. For run HICO2:23, with elevated CO_2 and present obliquity, Earth is warm and relatively snow- and ice-free to begin with, and tilting the planet further only cools the planet by depressing insolation and temperatures in the tropics. Thus, the global annual-mean temperature cycles for runs HICO2:54–HICO2:85 in Fig. 13 all lie beneath the cycle for HICO2:23. The amplitudes of the seasonal cycles for the HICO2 runs are also a few degrees smaller than for the PRES runs because the heavy CO_2 blanket prevents low-insolated areas during winter from cooling to the same degree that they do under skies of greater transparency.
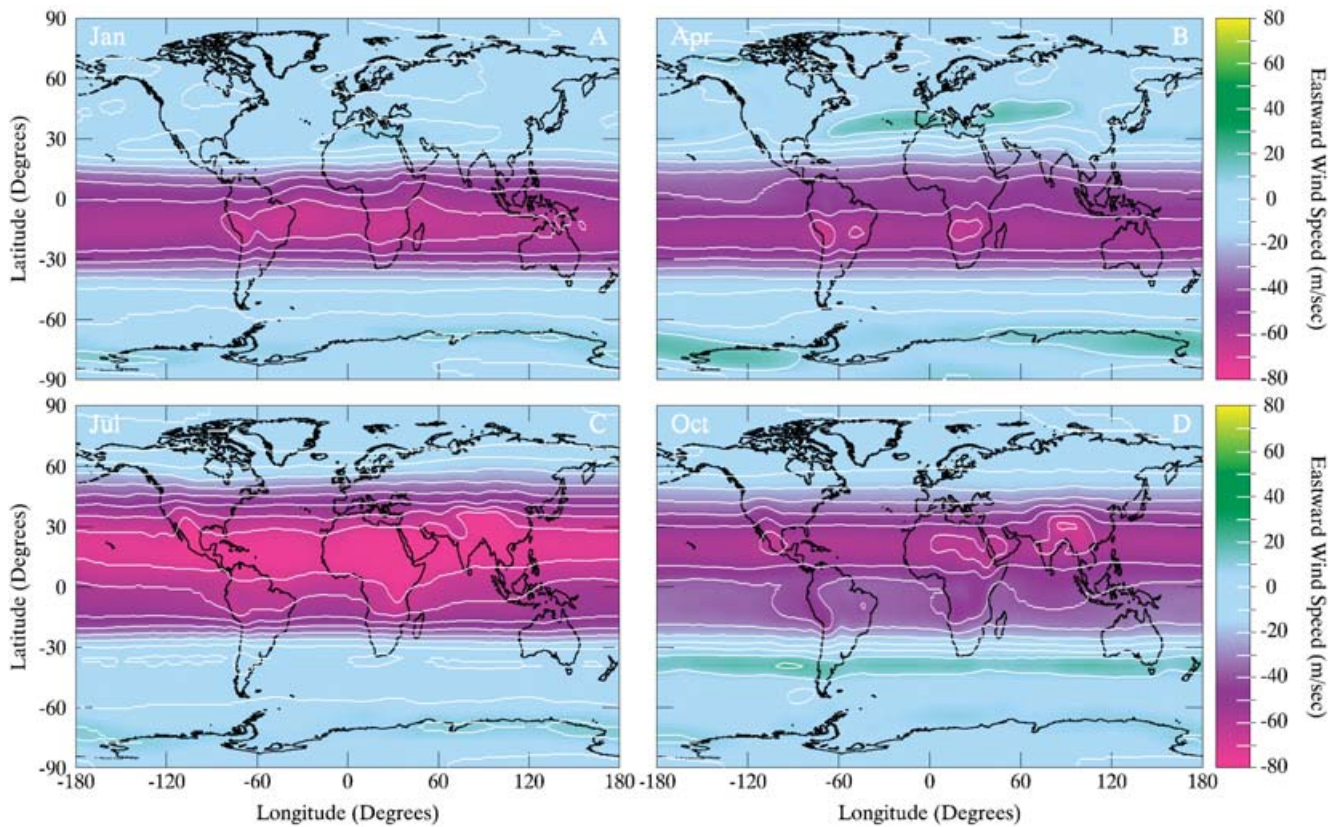
Fig. 12. Monthly mean eastward wind speed in m s^{-1} at a sigma level (P/P_0) of 0.251, or a height of ~ 10 km above the surface, for run PRES85. Compare with Fig. 6.

As an example of the extreme temperatures that are possible with elevated CO_2, we show here four global temperature maps for run HICO2:85 in Fig. 14, which are best compared with the maps for run PRES85 shown in Fig. 9. The most significant differences between the two runs are a slight ($\sim 2\%$) increase in planet surface area with temperatures above 50 °C for the month of July, and the warmer tropical oceans which keeps areas near the equator free of snow most of the year, despite the reduced insolation.

Climate simulations at zero obliquity

The last major glaciation in Earth's history reached its maximum 21 kyr ago covering northern America and northern Europe with ~ 3 km of ice (Peltier 1994). This 'ice age' was in part enabled by anomalously low levels of the greenhouse gases CO_2 and CH_4 (Kump *et al.* 1999), but it may also have been influenced by Milankovitch orbital insolation forcing, which reduced polar temperatures ~ 25 kyr ago promoting glacial advance. A natural question is, 'to what degree would Earth or other Earth-like planets be affected by glaciations if their obliquities were much smaller than Earth's is today?' We chose to address this issue here by reducing Earth's obliquity to 0°, while holding all run parameters (except geography) equal to their present values. We used two different geographies, present and Sturtian (after the Late Proterozoic period ~ 750–720 Ma), to see how the growth of ice sheets is affected by the size and locations of continents.
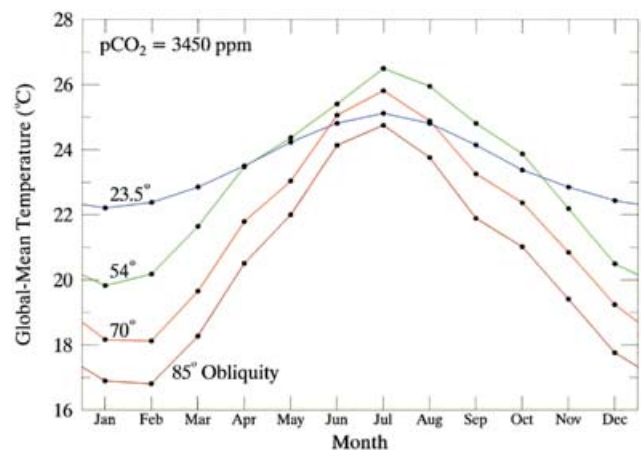

Fig. 13. Seasonal variation of global-mean temperature (in °C) for the present Earth with elevated CO_2 (3450 ppm) and with several different obliquities. Runs graphed here include HICO2:23 (23.5° obliquity), HICO2:54 (54°), HICO2:70 (70°) and HICO2:85 (85°) using the colours blue, green, orange and red, respectively.

The names of the two zero-obliquity runs are PRES0 and STUR0, respectively.

Even though the obliquity is zero for both runs, there is a very small seasonal cycle (not shown) with a peak-to-peak amplitude of ~ 0.7 °C owing to the slight variation in Earth's distance from the Sun in its eccentric orbit ($e = 0.0167$). The
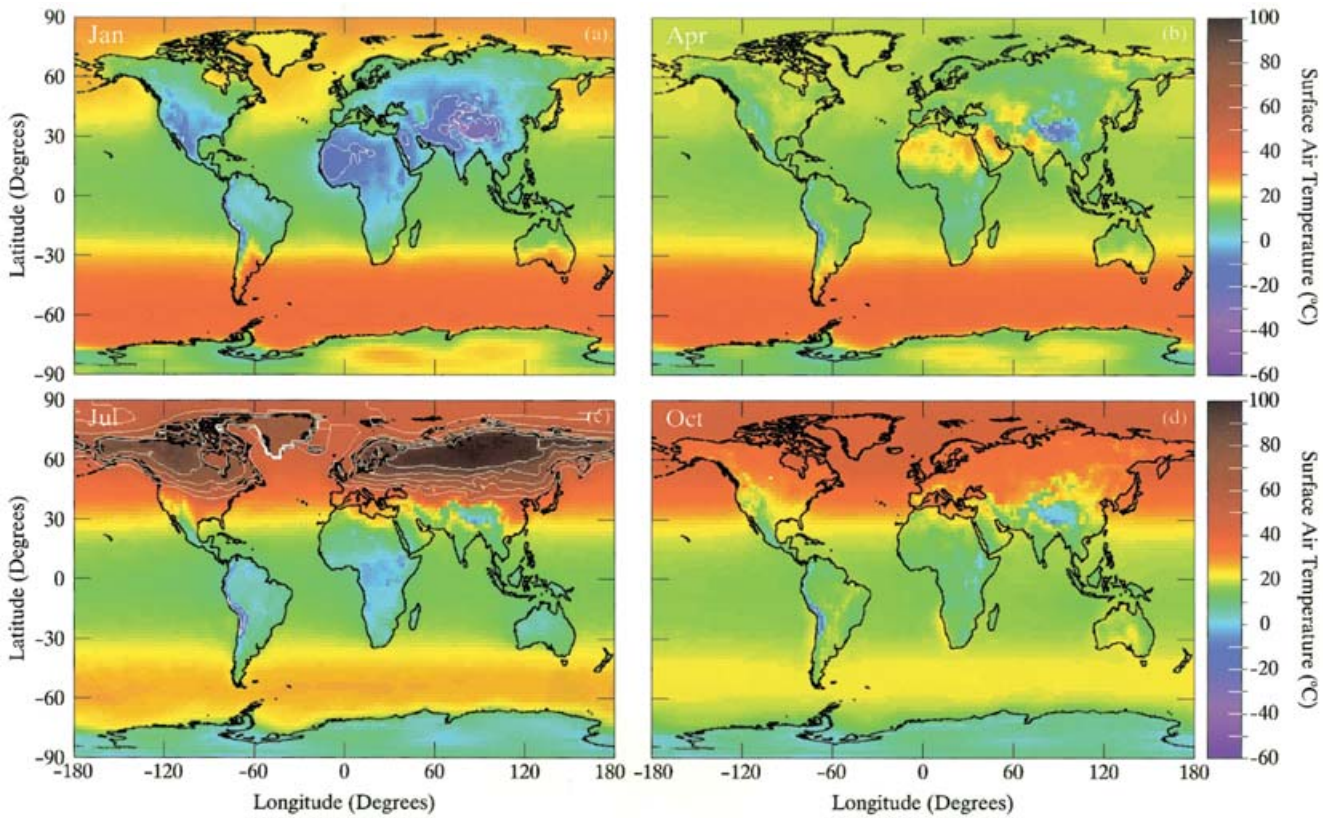
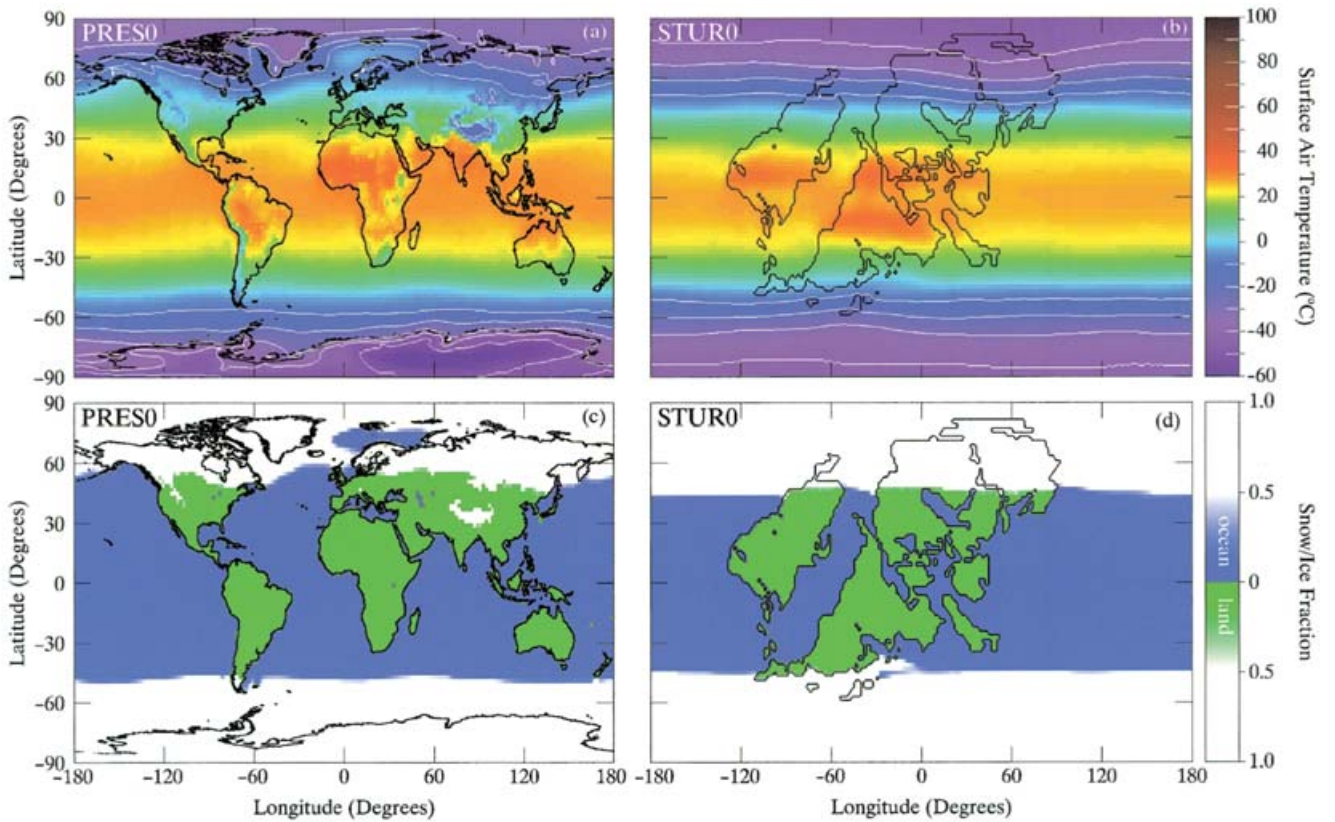**Fig. 14.** Monthly mean 2 m surface air temperatures (°C) for run HICO2:85. Compare with Figs 3 and 9.

Fig. 15. January monthly mean 2 m surface air temperatures (°C) and the distribution of ice and snow for runs PRES0 and STUR0. Only one month is shown here because of the absence of a significant seasonal cycle at zero obliquity.
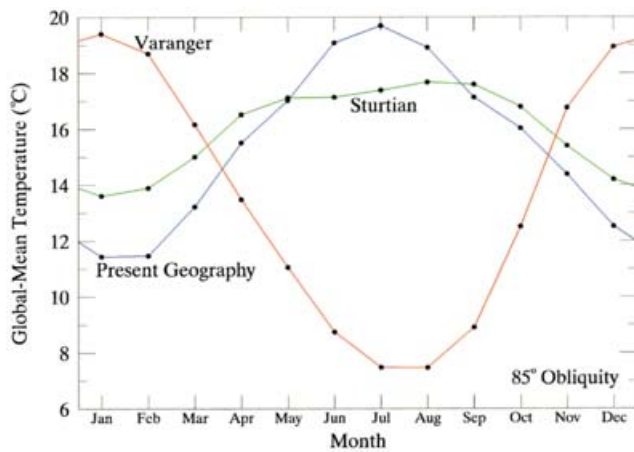
Fig. 16. Seasonal variation of global-mean temperature (in °C) at 85° obliquity for three different geographies: (i) run PRES23 with the present geography (blue); (ii) run STUR85 with Sturtian geography (green); and (iii) run VARA85 with Varanger geography (red).

highest temperatures in the cycle occur in January when the Earth is closest to the Sun. Seasonal changes to the other climate parameters (e.g. snow and ice cover, precipitation, wind speed) are also small, so we only show single global maps for the two most important data elements: surface temperature and the distribution of ice and snow (Fig. 15). Fig. 15(b) shows global ice and snow coverage for run PRES0. The ice line in both hemispheres extends to within 50° of the equator, or approximately 20° further than the maximum ice extension on the present Earth. We assumed before running the GCM that ice would cover Greenland and Antarctica as today, but ice sheets will also likely form anywhere there is land that is covered with snow year round (e.g. Canada, Northern Europe and Siberia). An ice-sheet model is needed to accurately simulate the growth of new ice sheets from the GCM data but no such calculations were performed for these runs.

Two features of the snow–ice map bear further attention. First, there is an island of open ocean, possibly covered by thin or broken ice floes, that persists over the Barents Sea just north and west of Scandinavia. This 'island' is common to our two runs with present geography and significant polar sea-ice (i.e. PRES23 and PRES0), and results from the inclusion of an *ad hoc* increase in the slab ocean heat convergence parameter into a specified rectangle in the Norwegian Sea. The enhancement is needed to keep this region ice-free as observed for the present Earth (PRES23). (In reality, the sea is kept ice-free by deep ocean currents and very little stratification in that region of the planet. There is little guarantee, however, that the Norwegian sea would actually remain unfrozen at zero obliquity given that the deep-ocean circulation might be very different for runs PRES23 and PRES0.)

The second thing to note about Fig. 15(b) is the extent of the snow–ice coverage over northern America, northern Europe and Siberia. The snow–ice line over North America reaches the Great Lakes, where ice is thought to have reached

21 kyr ago with Earth at a much higher obliquity, but the land area potentially affected by glaciations (i.e. land with permanent snow cover) for run PRES0 is more than five times the area of the sheets covering the northern hemisphere during the last glacial advance.

For run STUR0 with predominantly equatorial (Sturtian) geography, the snow–ice line is shown to extend to within $\sim 40°$ of the equator (Fig. 15d). This is mainly due to differences in continental surface area; with present geography, 31.4% of the planet's surface is covered by land compared with 22.9% for Sturtian geography. The smaller continents near the equator for run STUR0 allows the tropics to be slightly cooler than the tropics in run PRES0 (compare Figs 15a and c), which allows the high-latitude ice to expand. The global annual-mean temperatures listed in Table 1 support this idea. The average temperatures for runs PRES0 and STUR0 are 11.2 and 7.2 °C, respectively. Nearly a quarter of the planet in run STUR0 has a temperature below -10 °C, compared with only $\sim 15\%$ for run PRES0 (as will be shown graphically in Fig. 24 later).

Equatorial versus Polar geography at high obliquity

For the final pair of runs, STUR85 and VARA85, we used paleogeographic reconstructions for the Precambrian Earth to test the extremes of climate that are possible on planets with different continental configurations. The two geographic reconstructions represent two times during the Late Proterozoic era, approximately 750 and 540 Ma, respectively (Lawver *et al*. 1999). The 750 Ma reconstruction coincides with the recognized Sturtian glaciation (~ 750–720 Ma). However, the 540 Ma reconstruction does not coincide exactly with the recognized Varanger glaciation (~ 610–575 Ma), but this was the closest reconstruction available to us, and our GCM simulations using it are termed 'Varanger' below. Sturtian geography was used previously in the zero-obliquity run, STUR0, and has 75% of its land area within 40° of the equator (compared with 58% for the present Earth). By contrast, Varanger geography has 57% of its continental surface area within 40° of the equator, with the remaining 42% surrounding the southern pole.

Both runs were performed with the second purpose of simulating Earth's climate during the Precambrian (at different obliquities) when the Sun was slightly less luminous than today (0.94 $L_\odot$). In addition to changing solar luminosity, we somewhat arbitrarily set pCO₂ for both runs equal to 420 ppm (Table 1), although the actual level for that time could have been very different from this value. This value for pCO₂ works to offset some of the cooling resulting from the reduced solar luminosity and so makes it easier to compare the results of these runs with earlier runs using the present-day Sun. (The reader is cautioned, however, that elevated pCO₂ and reduced solar luminosity are *not* in perfect balance here. Our planets are actually slightly colder than those at present pCO₂ and with a normal Sun, assuming all other run parameters are identical.)

Simulations STUR85 and VARA85 were both run at 85° obliquity, but they yielded dramatically different outcomes.
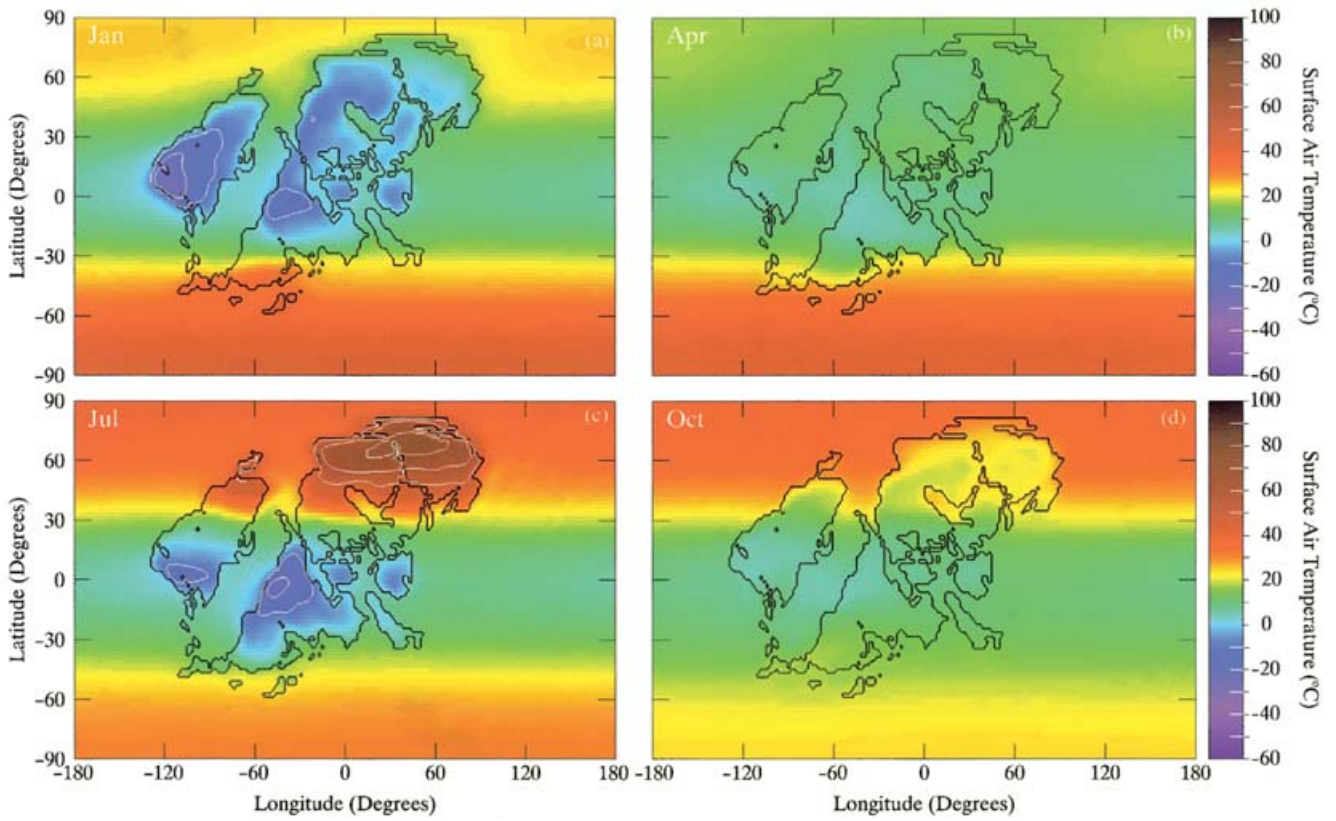
Fig. 17. Monthly mean 2 m surface air temperatures (°C) for run STUR85 with continents situated primarily at low latitude.
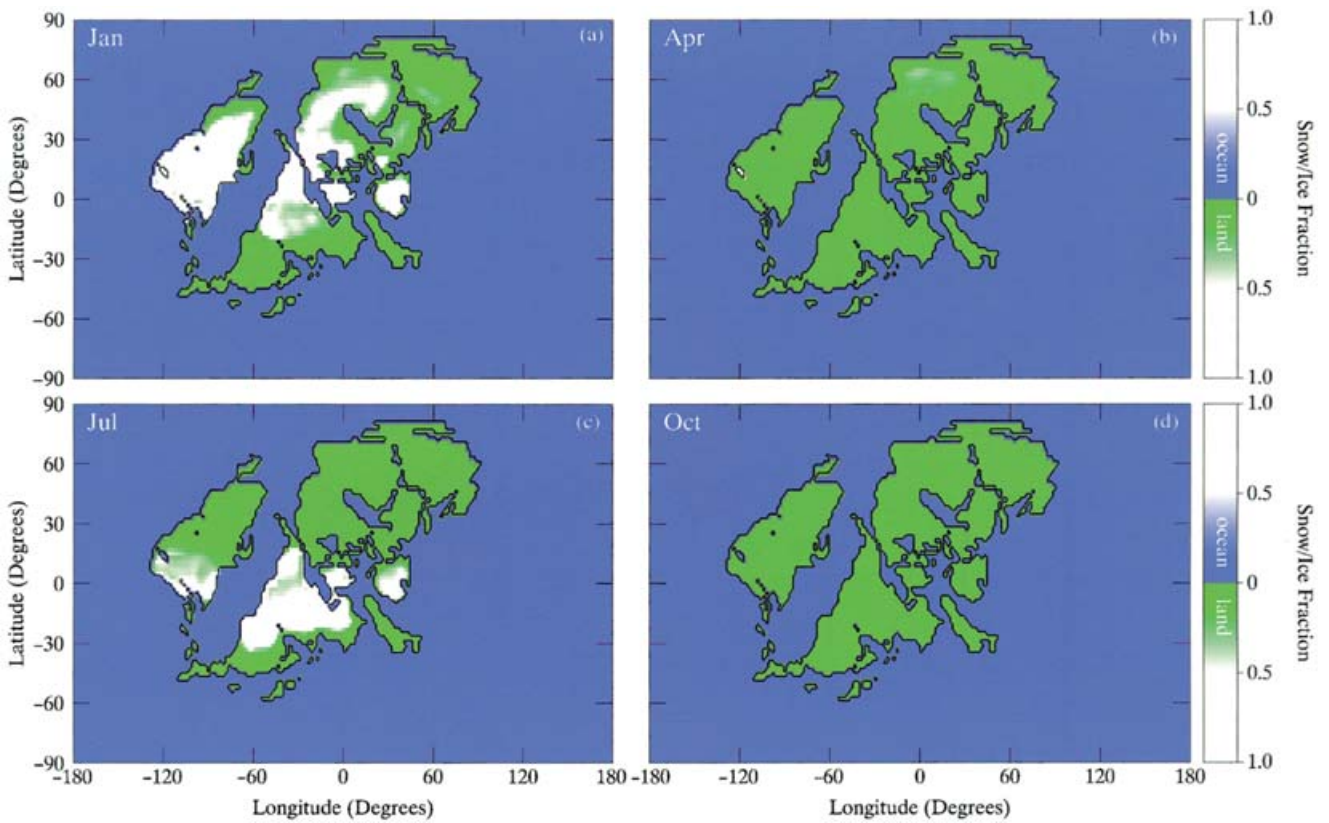
Fig. 18. Seasonal distribution of ice and snow with Sturtian geography for run STUR85.
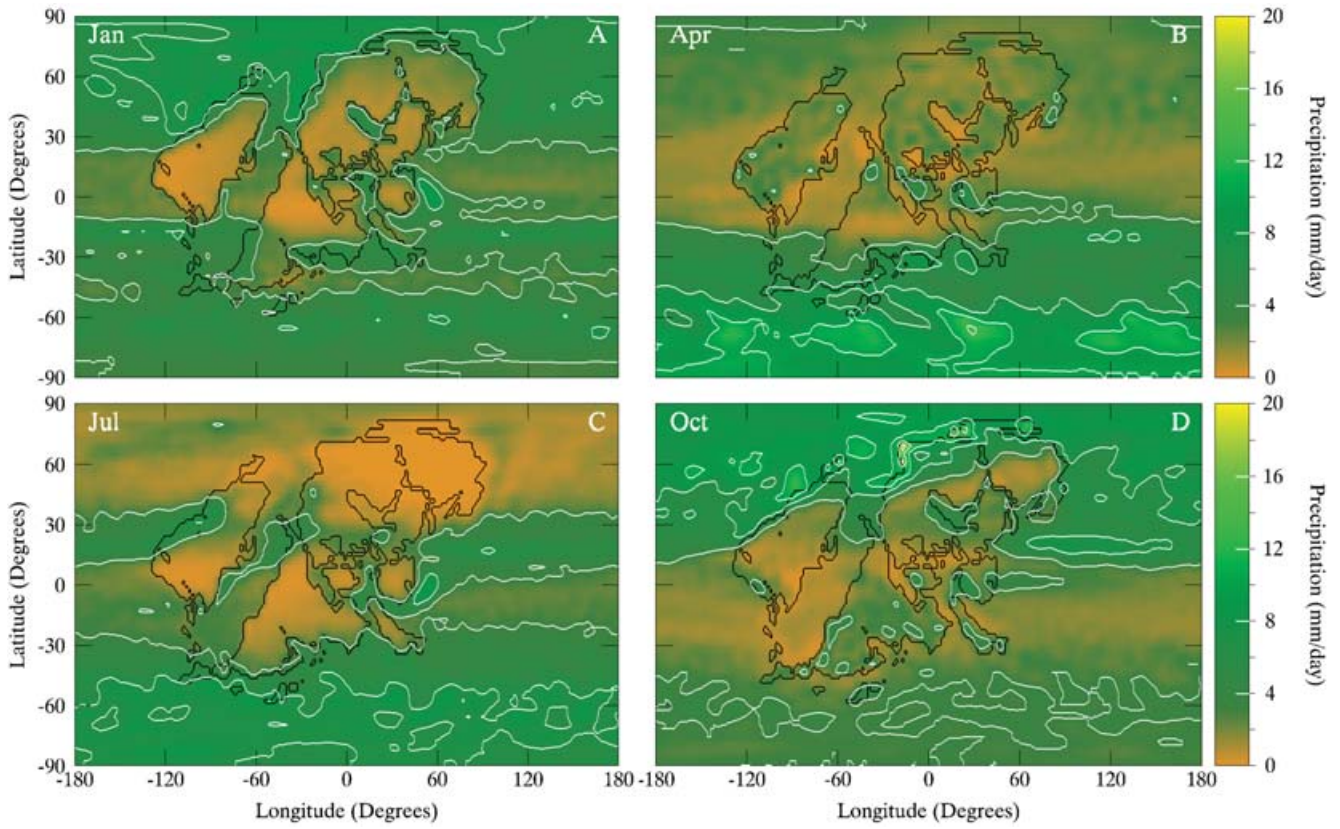
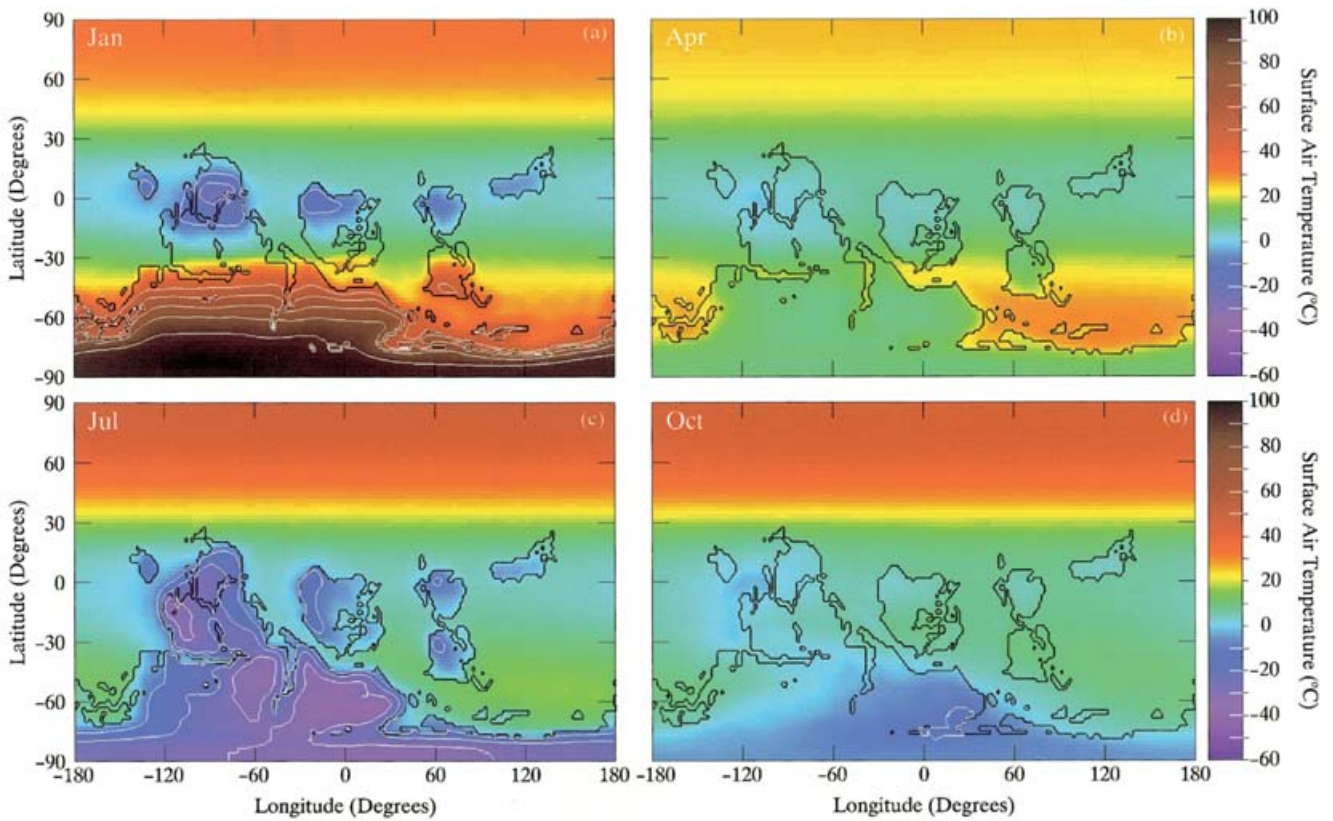**Fig. 19.** Monthly mean precipitation in mm d^{-1} for run STUR85.

Fig. 20. Monthly mean 2 m surface air temperatures ($^{\circ}$C) for run VARA85 with continents situated primarily at high latitude.
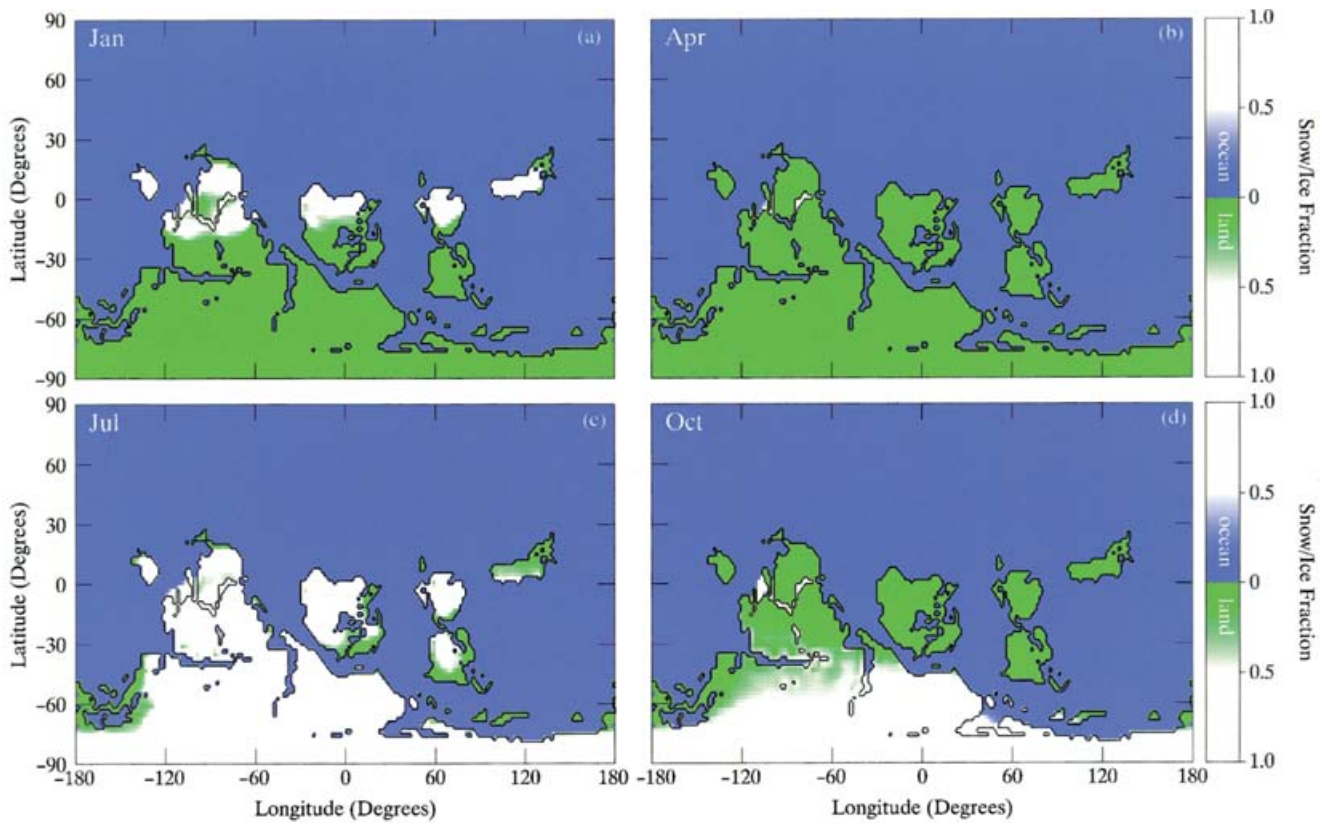
Fig. 21. Seasonal distribution of ice and snow with Varanger geography for run VARA85.

The extraordinary nature of these results warrants displaying them in full detail, so we include here seasonal maps of surface temperature, snow and ice coverage, and precipitation. Global wind patterns are not shown because they closely resemble each other and that of the earlier high-obliquity runs, with strong (>60 m s^{-1}) winds blowing aloft to the west.

Global-mean seasonal temperature cycles for both runs are shown in Fig. 16 along with the seasonal cycle for another run with the same high obliquity, PRES85, with present geography for comparison. Of the three runs shown, the variation in global-mean temperature is smallest (13–17 °C) for run STUR85, which is comparable to the cycle exhibited by the present Earth at 23.5° obliquity. The reason for the small amplitude is that the continents are located primarily at low latitude where the amplitude of the seasonal-insolation cycle is smallest at any obliquity (see Fig. 1). Thus, not every planet at high obliquity will exhibit large-amplitude seasonal temperature cycles. Global temperature maps for run STUR85 are shown in Fig. 17, and snow/ice cover and precipitation maps are given in Figs 18 and 19, respectively. In Fig. 17, we see that temperatures are coldest over continents within the tropics, as expected, but it is not cold enough to permit snow year round (see Fig. 18) or for glaciers to form at sea level. But snow could conceivably fall year round at higher elevation. Sea-level temperatures between 5 and 10 °C in April and October suggest that snow and ice might exist year round over continents with elevations exceeding 1–2 km, which would yield a successful explanation for the low-latitude

glacial paradox described earlier. It is also important to note that the warmest temperatures of the run are ~ 70 °C, which is 20–30 °C less than the maximum temperatures occurring over Siberia in run PRES85. This difference is partly a consequence of the smaller solar luminosity used here and partly a consequence of the smaller continental surface area located at high latitude for the Sturtian reconstruction.

Switching to the predominantly polar Varanger geography for run VARA85 nearly triples the amplitude of the global-mean seasonal cycle (see Fig. 16), and shifts the phase of the cycle by $\sim 180°$. Both the phase shift (relative to present and Sturtian geography) and amplification of the seasonal temperature cycle are a consequence of the high concentration of land around the southern pole, which responds rapidly to the extremely variable insolation at high obliquity. The planet simulated in this run would be the most hostile to life because over half of the continental surface area (covering 24.1 % of the entire planet) has temperatures that fall below -10 °C or climb above 50 °C (see Figs 23 and 24 later) around the solstices, and the planet oscillates seasonally between these high- and low-temperature extremes. Equally extraordinary is the large temperature gradient (>120 °C) between the equator and the pole in January, which enables temperatures to reach the boiling point of water near the pole while blizzards of snow fall in the tropics only a few thousand km away!

As with the STUR85 run, all continental surfaces are at sea level, and yet temperatures in the tropics are slightly cooler for run VARA85 than with STUR85. Once again, this results
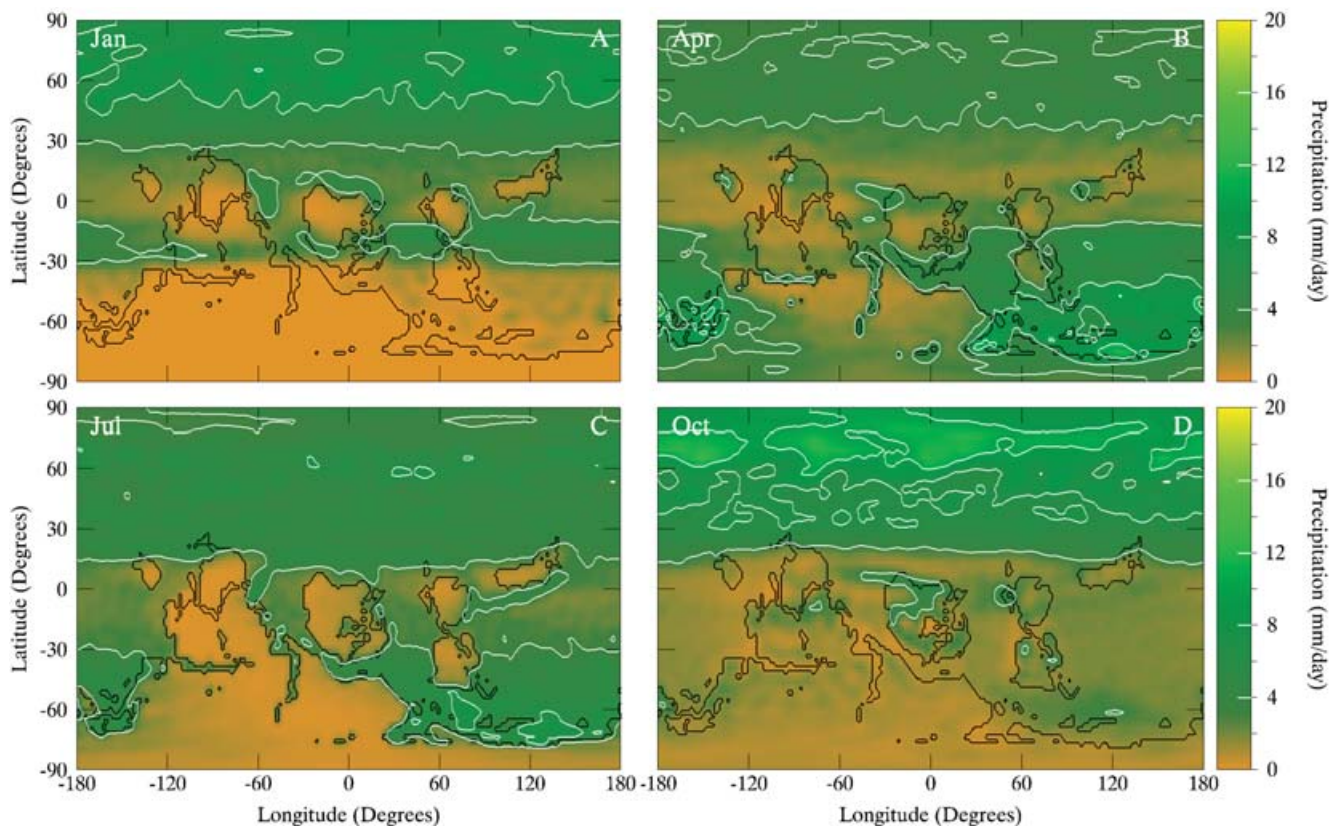
Fig. 22. Monthly mean precipitation in mm d^{-1} for run VARA85.

from the large land mass concentrated at high latitude for run VARA85 (see Fig. 20). Extremely cold air masses over the polar supercontinent around July cool the entire southern hemisphere, which depresses temperatures in the tropics year round. The cold tropical ocean water keeps the smaller land masses clustered around the equator cold through the hot southern-hemisphere summer. In contrast, the atmosphere over the slowly varying waters surrounding the northern pole oscillates only between 25 and 40 °C because of the absence of land.

In July, snow covers more than 75% of the total continental surface area (see Fig. 21) despite the reduced precipitation in these areas during the coldest months (see Fig. 22). Delivery of moisture to the centre of the polar supercontinent is accomplished here by winds blowing off the oceans around the time of the equinoxes when the tropics are warmest. The efficiency of moisture delivery is very different from the present Earth where the relatively small polar continent of Antarctica remains virtually dry year round even though it is surrounded by a large band of open water. As in runs PRES85 and HICO2:85, the entire southern hemisphere dries out completely when temperatures reach their highest levels around the summer solstice.

Fig. 21 shows that snow is unable to exist year round at sea level in the tropics, as was true for run STUR85. The absence of year-round snow cover in the tropics at sea level for both this run and run STUR85 weakens the idea that low-latitude glaciation on Earth during the Late Precambrian was

somehow initiated by high obliquity, but there is certainly lots of room for further modelling. Our simulations suggest that achieving low-latitude glaciation may not be difficult at high elevations or with CO_2 levels lower than those assumed here.

Conclusions

Planetary habitability

When Laskar and colleagues (Laskar *et al.* 1993) first suggested that episodes of high obliquity might render the Earth uninhabitable, they were most likely imagining a planet with either superheated continents or frozen landmasses covered by ice and snow. Indeed, both extremes are realized in the extraordinary case of run VARA85. Yet, the term 'habitable' has been historically applied to any Earth-like planet or moon whose climate allows liquid water to exist somewhere on its surface over at least a portion of its orbit (cf. Kasting *et al.* 1993; Williams & Kasting 1997; Williams & Pollard 2002). On the most liberal front, a world is 'habitable' if it is not so warm that it succumbs to a runaway greenhouse or so cold that it experiences irreversible global refrigeration. All of the planets simulated here are 'habitable' according to this broad definition because even the most extreme values of obliquity are not enough to initiate a climatic catastrophe (although this possibility is not ruled out for other worlds not considered here). Generally speaking, global annual-mean temperature is only weakly dependent on obliquity because the global annual-mean stellar flux received
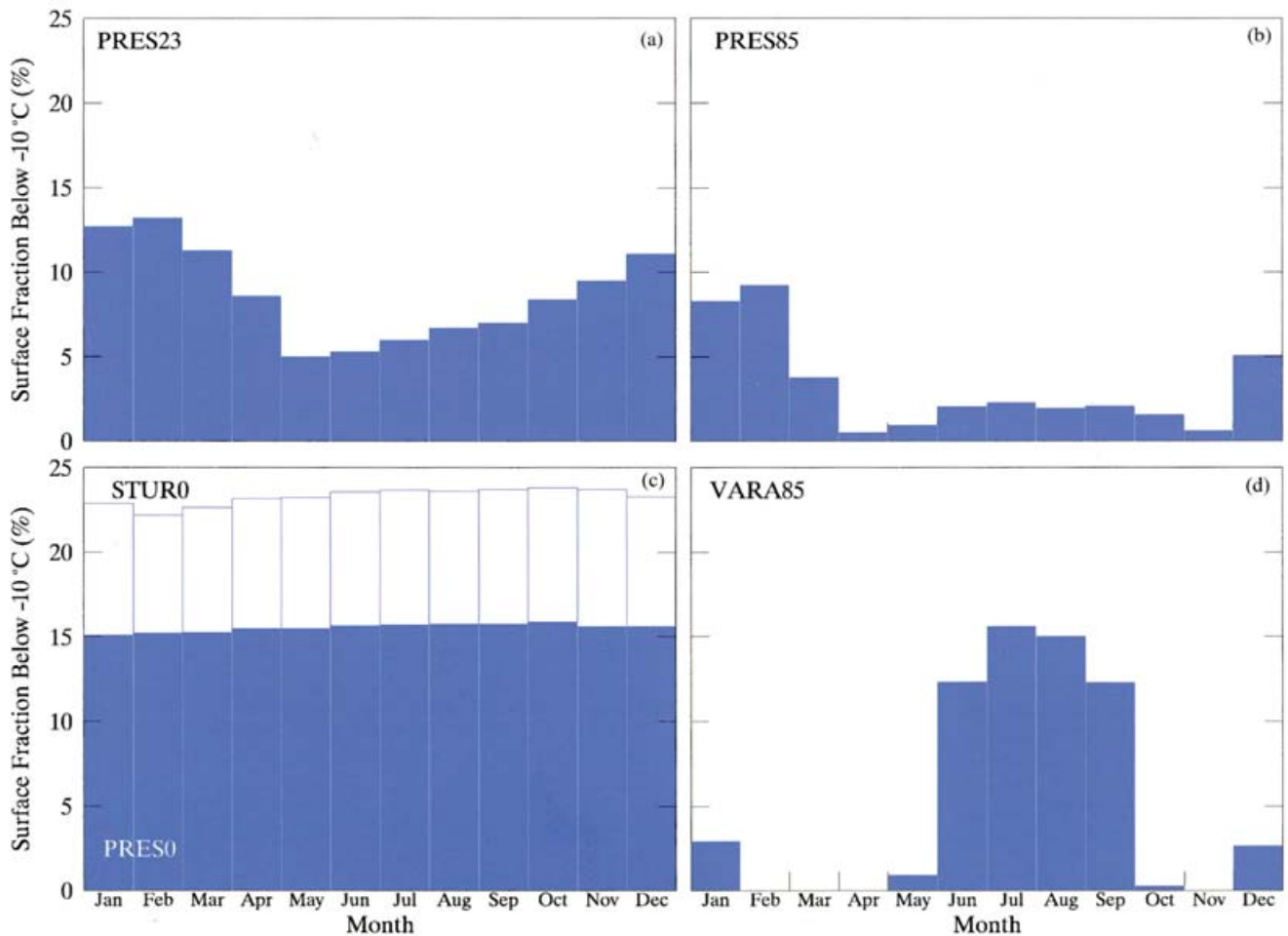
Fig. 23. Seasonal variation of the global surface fraction with temperatures below $-10\,^{\circ}$C for runs (a) PRES23, (b) PRES85, (c) PRES0 (filled) and STUR0 (open) and (d) VARA85.

by a planet is the same (equal to $Q_0/4$, where Q_0 is the flux from the parent star), regardless of how the planet's spin axis is oriented in space.

If we narrow our habitability criterion slightly to include only those areas of a planet with temperatures between, say, -10 and $50\,^{\circ}$C, we can now determine what fraction of a planet is 'habitable' at a given moment and what fraction is 'habitable' when averaged over the entire seasonal cycle. Figs 23 and 24 show the percentage of a few select planet surfaces where temperatures are either below $-10\,^{\circ}$C or above $50\,^{\circ}$C. According to Fig. 23, present Earth (run PRES23) is one of the most uninhabitable planets that we have simulated. Approximately 8.7% of Earth's surface is colder than $-10\,^{\circ}$C on average, and this percentage peaks at 13.2% in February owing to the large landmasses at high latitude covered by snow. The only planets that are appreciably colder than the present Earth are those simulated in the zero-obliquity runs PRES0 and STUR0. For run PRES0 with present continents, 15.6% of the planet is colder than $-10\,^{\circ}$C on average. In contrast, planet STUR0 with smaller continents situated primarily at low latitude has a mean temperature of only $7.2\,^{\circ}$C, and 23.3% of its surface area is below $-10\,^{\circ}$C.

As mentioned earlier, run VARA85 is seasonally the most peculiar. Fig. 23 shows that 15.6% of its surface (or $\sim65\%$ of its land area) drops below $-10\,^{\circ}$C in July. Six months later in January, 9.3% of its surface reaches temperatures above $50\,^{\circ}$C (Fig. 24). The temperature extremes are reduced somewhat around the time of the equinoxes when the sun is over the equator, but when the extreme solstice temperatures are averaged over the seasonal cycle, nearly 7% of this planet's surface ($\sim28\%$ of its land area) is outside the 'habitable' range of temperatures. This simulation suggests that planets with either large polar supercontinents or with small inventories of water will be most problematic for life at high obliquity.

All of the other runs performed for this study are warmer than the Earth owing to the high temperature spike affecting the high-latitude continents around the summer solstice. The intense summer heating of both hemispheres works to keep the surface and atmosphere warm during the prolonged, dark winter months. Warming of Antarctica and the surrounding ocean between November and February in run PRES85, for example, keeps the continent snow-free year round even during the long Antarctic winter. (Fig. 9 shows that
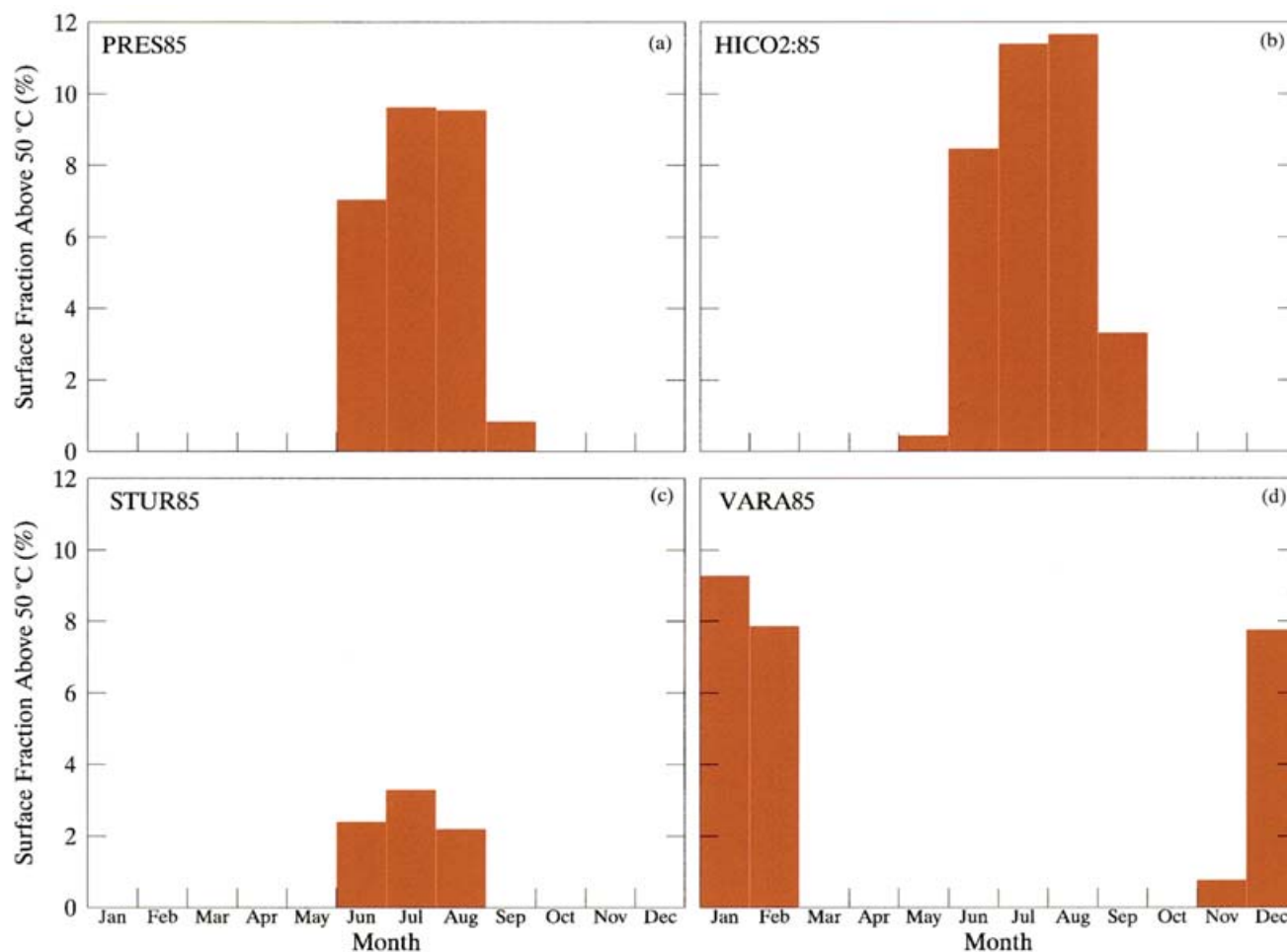
Fig. 24. Seasonal variation of the global surface fraction with temperatures above 50 °C for runs (a) PRES85, (b) HICO2:85, (c) STUR85 and (d) VARA85.

Antarctica is actually this planet's best location for water-dependent life because of the clement temperatures and small seasonality.) Contrary to initial expectation, none of our simulated planets exhibited permanent ice sheets near the equator at high obliquity. This indicates that the low-latitude glaciations appearing on Earth near sea level during the Late Precambrian may not have been caused by high obliquity, although such cases have been found by Ogelsby & Ogg (1998) and Jenkins (2000) with somewhat different boundary conditions.

The absence of permanent ice cover does not by itself guarantee that a world is suitable for life. The high-temperature extremes exhibited in most of our runs would be problematic for all but the simplest life forms on Earth today. Photosynthetic organisms would be challenged by the long periods of darkness that would affect nearly an entire hemisphere for months. Some of our planets might only be suitable then to a class of organisms known on Earth as extremophiles, which occupy the dark ocean bottom or deep underground and which can withstand temperatures approaching 400 °C, provided they are near a source of water. Such organisms would easily withstand the temperature

variations of extraordinary amplitude that we have simulated here.

Could our planets support more advanced life at high obliquity? Our results show that the answer to this question is yes provided the life does not occupy continental surfaces plagued seasonally by the highest temperatures. The case of run HICO2:85, our warmest planet, shows that nearly 12% of the planet is above 50 °C in July, but this is only 40% of the land area available to life (and 17% of the area available to marine life). And while such worlds exhibit climates that are very different from Earth's (indeed, they are extraordinary!), many will still be suitable for both simple and advanced forms of water-dependent life. On these theoretical grounds, then, Earth-like planets with high obliquities need not be eliminated from future searches for life beyond the solar system.

Acknowledgments

which our Sturtian and Varanger GCM maps were made. Our climate runs were performed on CRAY supercomputers belonging to the National Center for Atmospheric Research and the Environment Institute of the College of Earth and Mineral Sciences at the Pennsylvania State University. D.W. and D.P. were supported by a grant from the NSF/NASA-sponsored LExEn (Life in Extreme Environments) Program awarded in 1999.

Additional information

Images and animations of the model results may be viewed at http://shahrazad.bd.psu.edu/Williams/LExEn/main.html

References

Agnor, C.B., Canup, R.M. & Levison, H. (1999). On the character and consequences of large impacts in the late state of terrestrial planet formation. *Icarus* **142**, 219–237.

Alexandre, C.M. & Laskar, J. (2001). The four final rotation states of Venus. *Nature* **411**, 767–770.

Canup, R.M. & Agnor, C.B. (2000). Accretion of the terrestrial planets and the Earth–Moon system. In *Origin of the Earth and Moon*, eds Canup, R.M. & Righter, K., pp. 113–132. University of Arizona Press, Tuscon, AZ.

Chandler, M.A. & Sohl, L.E. (2000). Climate forcings and the initiation of low-latitude ice sheets during the Neoproterozoic Varanger glacial interval. *J. Geophys. Res.* **105**, 20 737–20 756.

Evans, D.A., Beukes, N.J. & Kirschvink, J.L. (1997). Low-latitude glaciation in the Palaeoproterozoic era. *Nature* **386**, 262–266.

Hoffman, P.F., Kaufman, A.J., Halverson, G.P. & Schrag, D.P. (1998). A Neoproterozoic snowball Earth. *Science* **281**, 1342–1346.

Hunt, B.G. (1982). The impact of large variations of the Earth's obliquity on the climate. *J. Meteor. Soc. Japan* **60**, 309–318.

Hyde, W.T., Crowley, T.J., Baum, S.K. & Peltier, W.R. (2000). Neoproterozoic 'snowball Earth' simulations with a coupled climate-ice sheet model. *Nature* **405**, 425–429.

Jenkins, G.S. (2000). Global climate model high-obliquity solutions to the ancient climate puzzles of the faint-young Sun paradox and low-latitude Proterozoic glaciation. *J. Geophys. Res.* **105**, 7357–7370.

Jenkins, G.S. (2001). High obliquity simulations for the Archaen Earth: implications for climatic conditions on early Earth. *J. Geophys. Res. (Planets)* **106**, 32 903–32 913.

Jenkins, G.S. (2003). GCM greenhouse and high-obliquity solutions for early Proterozoic glaciation and middle Proterozoic warmth. *J. Geophys. Res. (Atmos)* **108**(D3), 4118.

Kasting, J.F. (1992). Proterozoic climates: the effect of changing atmospheric carbon dioxide concentrations. In *The Proterozoic Biosphere: a Multidisciplinary Study*, eds Schopf, J.W. & Klein, C., pp. 165–168. Cambridge University Press, Cambridge.

Kasting, J.F., Whitmire, D.P. & Reynolds, R.T. (1993). Habitable zones around main sequence stars. *Icarus* **101**, 108–128.

Kump, L.R., Kasting, J.F. & Crane, R.G. (1999). *The Earth System*. Prentice-Hall, Upper Saddle River, NJ.

Laskar, J. & Robutel, P. (1993). The chaotic obliquity of the planets. *Nature* **361**, 608–614.

Laskar, J., Joutel, F. & Robutel, P. (1993). Stabilization of the Earth's obliquity by the Moon. *Nature* **361**, 615–617.

Lawver, L.A., Coffin, M.F., Dalziel, I.W.D., Gahagan, L.M. & Schmitz, R.M. (1999). The Plates 1999 Atlas of Paleogeographic Reconstructions (Plates Progress Report No. 235). University of Texas Institute for Geophysics Technical Report No. 187.

N'eron de Surgy, O. & Laskar, J. (1997). On the long term evolution of the spin of the Earth. *Astron. Astrophys.* **318**, 975–989.

Oglesby, R.J. & Ogg, J.G. (1998). The effect of large fluctuations in obliquity on climates of the Late Proterozoic. *Paleoclimates* **2**, 293–316.

Peltier, W.R. (1994). Ice age paleotopography. *Science* **265**, 195–201.

Pollard, D. & Thompson, S.L. (1995). Use of a land-surface-transfer scheme (LSX) in a global climate model: the response to doubling stomatal resistance. *Glob. Planet. Change* **10**, 129–161.

Thompson, S.L. & Pollard, D. (1997). Greenland and Antarctic mass balances for present and doubled atmospheric CO_2 from the GENESIS version 2 global climate model. *J. Climate* **10**, 871–900.

Ward, W.R., Agnor, C.B. & Canup, R.M. (2002). Obliquity variations in planetary systems. *Abstract for 33rd Lunar and Planetary Science Conf.*, Houston TX.

Williams, D.M. (1998a). The susceptibility of Earth-like planets to large obliquity variations. In *The stability of habitable planetary environments*, *PhD dissertation*, pp. 95–110. Pennsylvania State University.

Williams, D.M. & Kasting, J.F. (1997). Habitable planets with high obliquities. *Icarus* **129**, 254–268.

Williams, D.M., Kasting, J.F. & Frakes, L.A. (1998). Low-latitude glaciation and rapid changes in the Earth's obliquity explained by obliquity-oblateness feedback. *Nature* **396**, 453–455.

Williams, D.M. & Pollard, D. (2002). Earth-like worlds on eccentric orbits: excursions beyond the habitable zone. *Int. J. Astrobiol.* **1**, 61–69.

Williams, G.E. (1993). History of the Earth's obliquity. *Earth Sci. Rev.* **34**, 1–45.

Williams, G.E. & Schmidt, P.W. (1998). Paleomagnetism of the Palaeoproterozoic Gowganda and Lorrain formations, Ontario: low paleolatitude for Huronian glaciation. *Earth Planet. Sci. Lett.* **153**, 157–169.

Williams, G.P. (1988b). The dynamical range of global circulations – I. *Climate Dynam.* **2**, 205–260.

Williams, G.P. (1988c). The dynamical range of global circulations – II. *Climate Dynam.* **3**, 45–84.